Westinghouse ENGINEER

MARCH 1963

6939 A.D.

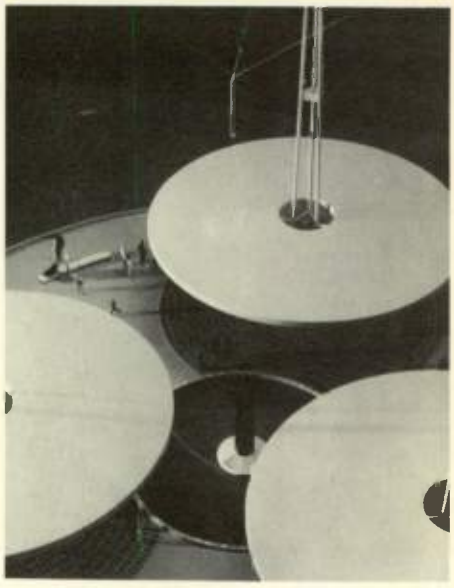

A new message to people 5000 years in the future will be buried at the 1964–65 New York World's Fair, alongside the original Westinghouse Time Capsule, which was lowered to rest 50 feet below ground on September 23, 1938, at the previous New York World's Fair.

The contents of the first capsule were selected to provide a record of the history, faiths, arts, sciences, and customs of civilization as it was in 1938. This message to the future was prepared with the cooperation of hundreds of persons including archeologists, engineers, physicists, historians, artists, and librarians.

However, man's accomplishments in the past 25 years have been perhaps the most important in history—particularly in the field of science. Our lives have been changed so significantly that the original Time Capsule, while it still records much of our present civilization, has become seriously out of date and would give the peoples of 6939 an inadequate picture of life in the 20th century. Among important accomplishments not included are atomic power, man in space, wonder drugs and polio vaccine, commercial television, and jet aircraft. Also unrecorded are World War II, the United Nations, the discovery of the Dead Sea Scrolls, and new data on the age of man and the earth.

A duplicate of the original Time Capsule will be on display at the open-air pavilion to be built by Westinghouse for the 1964–65 World's Fair. The capsule will be suspended between three pylons, 50 feet in the air directly above the eight-foot granite monument that marks the site of the original Time Capsule. A pool will reflect the image of the capsule in such a way that it appears to be at the depth of the buried capsule.

Contents of the duplicate capsule, which have been sealed inside since 1938, will be removed and put on public display in one of three open roofed areas at the base of the pylons. Exhibits under other pylons will contain materials selected for the new capsule, and a projection of life in the future.

Among the contents chosen for deposit in the 1938 capsule were some 35 articles of common use, ranging from a slide rule to a woman's hat, each selected for what it would reveal about us to archeologists fifty centuries hence. Also included were about 75 samples of representative materials ranging from fabrics, metals, alloys, plastics, and synthetics to a lump of anthracite coal and a dozen kinds of seed. Pages of books, articles, magazines, newspapers, reports, circulars, catalogs, and pictures were recorded on 3½ reels of microfilm. The printed material explains our arts, entertainments, religions, philosophies, educational systems, sciences, technology, and medicine. Also recorded on microfilm were messages to the future from three famous men: Dr. Albert Einstein, Dr. Robert Millikan, and Dr. Thomas Mann. The microfilmed material contains approximately 10 million words. A newsreel was added to show historic scenes of our times.

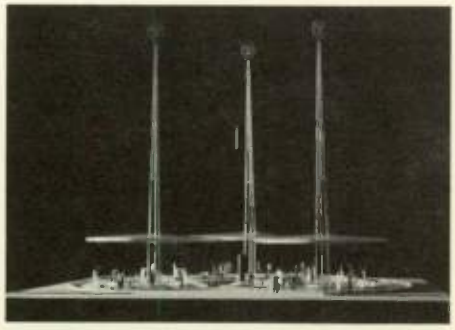

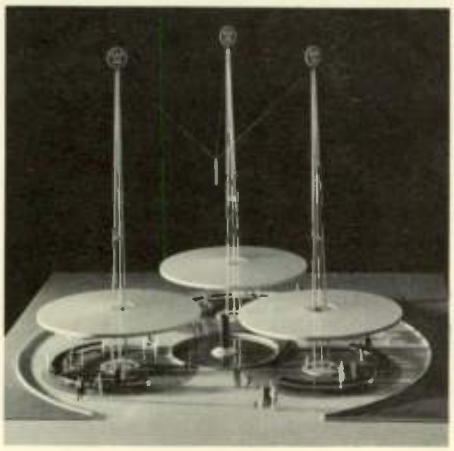

With the aid of representatives from the U. S. Bureau of Standards, all of these items were examined for durability to make certain that they would remain intact for 5000 years when enclosed in the capsule. Care was taken not to include any material that might produce fumes or acids capable of attacking other articles in the capsule. All liquids were ruled out and organic objects such as seeds were hermetically sealed in glass receptacles. The films were placed in aluminum containers lined with rag paper. All other objects were individually wrapped in heavy rag paper.

After packing the inner envelope of glass, the air inside was exhausted, replaced with nitrogen, and enough moisture injected to equal normal room humidity. Then the glass envelope was heated and sealed. This inner envelope of glass was placed in a Cupaloy shell, set in a water-repellent petroleum-base wax, and the cap of the capsule was secured to form an air-tight seal.

To insure that future generations would be able to locate the Time Capsule, a "Book of Record" was printed on permanent paper with special ink. More than 3000 copies of the publication were distributed to libraries, museums, monasteries, convents, lamaseries, temples, and other safe repositories throughout the world. Among other things, the book includes an ingenious key to the English language to aid archeologists of the future should knowledge of our present language be lost.

Selection of materials for the new capsule will again be handled by a special committee chosen from experts in the fields of science, industry, and education. The capsule will be made by Westinghouse of a special alloy and will resemble the original 7½-foot Time Capsule. At the closing of the World's Fair, it will rest beside the original capsule until both are recovered in 6939 A.D.

Westinghouse
ENGINEER
MARCH 1963

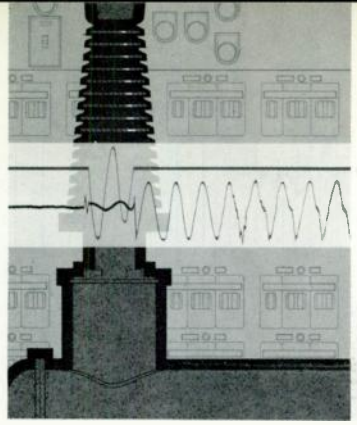

VOLUME 23 • NUMBER 2

Cover Design: High-power circuit breaker testing is the subject of this month's cover. Test oscillograms, an SF_6 breaker pole, and the panel of a sequence timer are the elements chosen by cover designer Thomas Ruddy of Town Studios, Pittsburgh.

The following terms, which appear in this issue, are trademarks of the Westinghouse Electric Corporation and its subsidiaries:

Thermalastic, Prodac, Tracpak, Westing-Arc, Cupaloy, Powercasting

Published bimonthly by the Westinghouse Electric Corporation, Pittsburgh, Pennsylvania.

Subscriptions: United States and Possessions, $2.50 per year; all other countries, $3.00 per year; single copies, 50¢ each.

Mailing address: Westinghouse ENGINEER, P. O. Box 2278, 3 Gateway Center, Pittsburgh 30, Pennsylvania.

Microfilm: Reproductions of the magazine by years are available on positive microfilm from University Microfilms, 313 N. First Street, Ann Arbor, Michigan.

Printed in the United States by The Lakeside Press, Lancaster, Pa.

Bigger Tests for Bigger Breakers

These higher capacity testing facilities at the Westinghouse high-power laboratories have been designed to meet the development demands of the future.

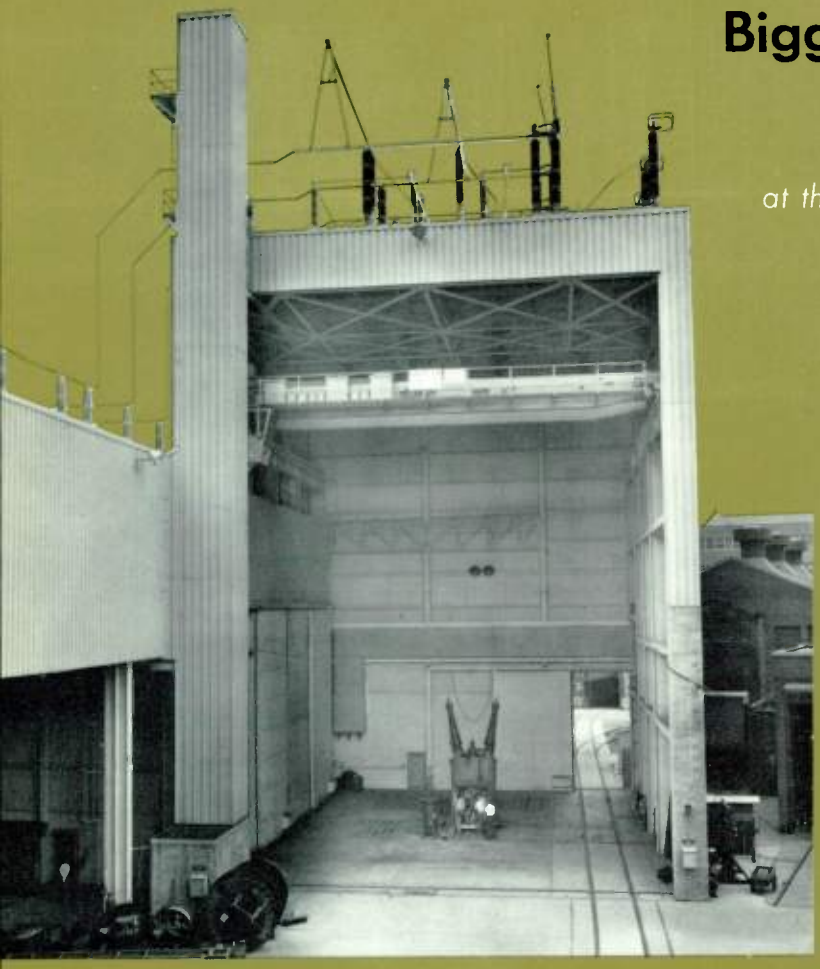

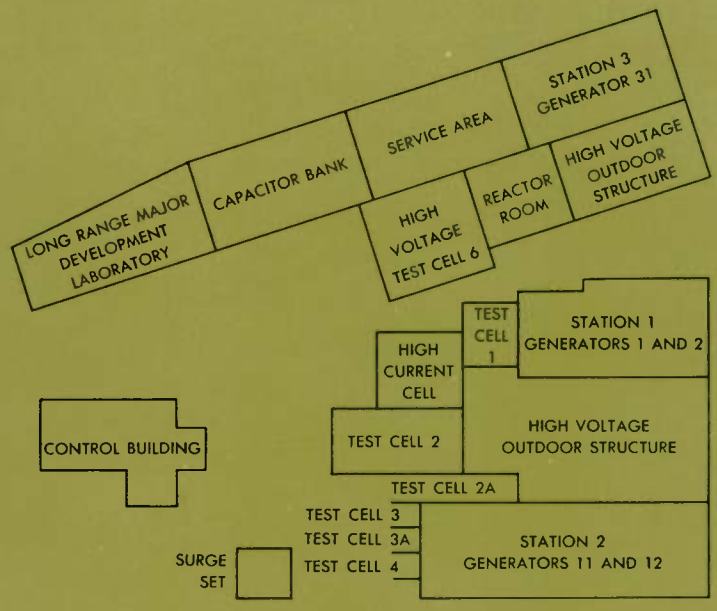

Fig. 1 The physical arrangement of the enlarged high-power testing laboratories.
Photo A view of one of the test cells.
Fig. 2 This schematic diagram shows the main power connections for the laboratory.

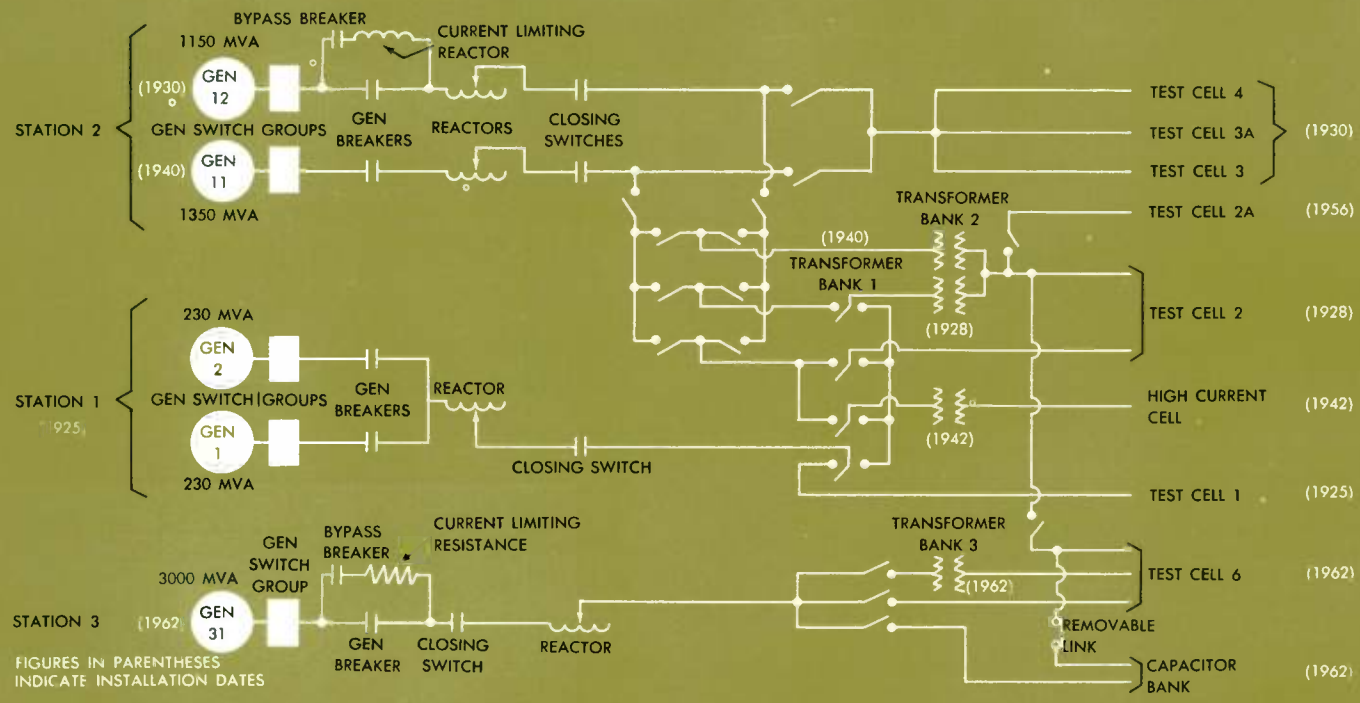

Advances in circuit breaker designs over the past four decades have depended to a large extent on exploratory work in the high-power testing laboratory. New design concepts will be required for circuit breakers of the future because of higher voltage transmission, and higher interrupting capacities will also be required. These new concepts will demand exhaustive testing during development.

Although the major use of the Westinghouse high-power laboratory is for developing and testing interrupting devices, it is also used extensively in the development of many other kinds of electrical equipment such as reactors, enclosed bus duct, transformers, and lightning arresters.

The higher capacity testing facilities now being put into service at the Westinghouse high-power testing laboratories at East Pittsburgh reflect the need for continued increases in circuit breaker ratings. Prior to 1962, the last significant increase in capacity was in 1940 when the second generator was installed in Station 2 and a second transformer bank was added. It is now deemed necessary to expand again, and a single-phase capacity of 2500 mva at transformer voltages was selected as the most logical step —an increase of 150 percent over the previous capacity. The 2500 mva output is obtained by paralleling Stations 2 and 3 at transformer voltages.

General Plan for New Laboratory

The arrangement of the complete laboratory facility is shown in Fig. 1. A single-line schematic of the entire group is shown in Fig. 2. The principal items included in the 1962 expansion are Station 3, which houses the new generator 31, a new transformer bank and high-voltage test cell, a new service area, and an additional capacitor bank.

The new high-voltage test cell (No. 6) can accommodate the largest breaker structures presently anticipated. The cell is 60 by 80 feet in floor area, 80 feet to the roof, and 50 feet to the crane hook. A large service area adjacent to this cell provides space for breaker assembly and adjustment before and during tests. Large trucks move equipment back and forth between the test cell and the service area. The generator room, reactor room, and transformer yard are all located nearby.

The capacitor bank is now located in a covered area adjacent to the test yard, and its capacity has been increased to 100 mva for line-dropping and capacitor switching tests at voltages up to 286 kv.

A separate test area has been provided for long-range circuit-breaker development. This area includes a small-scale testing facility and a machine shop for making and testing experimental models of new breaker concepts.

The new short-circuit generator (Fig. 3) is capable of delivering four successive short circuits in rapid sequence, each with an initial value of 3000-mva three phase, or 1500-mva single phase. These ratings correspond to symmetrical currents of 105 000 and 91 000 amperes respectively, but the generator is, of course, designed to withstand the effects of the fully asymmetrical peak currents of nearly 300 000 amperes. While the generator has no specified continuous load capacity, a nominal rating of 150

HISTORY OF CIRCUIT BREAKER TESTING

Prior to 1925, all short circuit tests on circuit breakers were made at the customer's facility. The range of currents and voltages were necessarily limited, and instrumentation was a problem since all setups were temporary. The need for a high-power testing laboratory at the manufacturer's plant was recognized in the early twenties, and led to the first high-power testing laboratory at the Westinghouse East Pittsburgh plant. The following tabulation shows the growth of these high-power testing facilities during the past four decades.

DATE	FACILITY INSTALLED	CAPACITY	
		Generator Voltage, Three Phase	Transformer Voltage, One Phase
1925	Station 1	400 mva	None
1928	Transformer bank 1	400 mva	175 mva
1930	Station 2—Generator 12	1150 mva	450 mva
1940	Generator 11 in Station 2, Transformer bank 2	[1]2500 mva	[2]1000 mva
1942	Cold room and high current transformer	200 000 amperes 3 phase 619 volts } 5 seconds 345 000 amperes 1 phase 619 volts } Cold room down to −20°F	
1955	Station 1 generators rewound	[5]460 mva	
1962	Station 3—Generator 31 Transformer bank 3	[3]3000 mva	[4]2500 mva
	Cold room increased	−40°F	

[1]Generator 11 and 12 in parallel
[2]Generator 11 and 12 in parallel, transformers in parallel or series
[3]Generator 31 only (no provision for paralleling at generator voltage)
[4]Station 2 and Station 3 in parallel, all transformers used
[5]Not paralleled with other generators

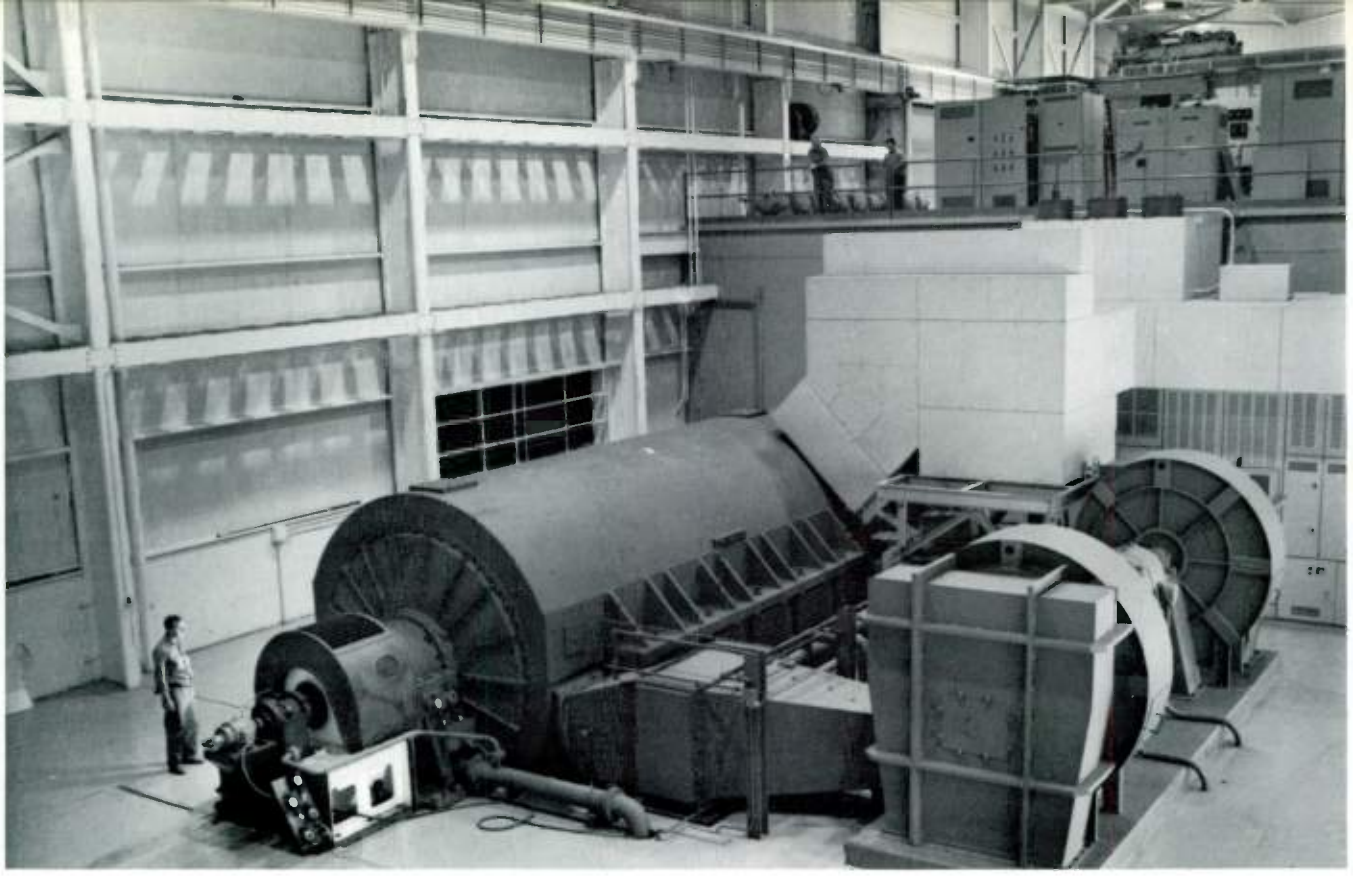

mva, 16.5 kv, was assigned as a base on which to make design calculations.

The generator is driven by a 1750-hp two-pole wound rotor induction motor. A liquid rheostat is used in the motor secondary to start the set in about 20 minutes and dynamic braking is provided to stop it in less than 15 minutes. Air-driven oil pumps are provided as backups for the motor-driven pumps in case of power failure.

Short-Circuit Generator Design

The design of a short-circuit generator differs considerably from the conventional central station machine. The principal function of a short-circuit testing generator—delivery of a large short-circuit kva—requires a machine with low reactance, relatively long time constants, and suited for superexcitation. It must be capable of operating either three phase or single phase, and of occasional operation at 25 or 50 cps. Therefore, although the generator looks much like a conventional turbine generator, it has many special features.

Low Subtransient Reactance—Since initial short-circuit current is limited by both transformer impedance and generator subtransient reactance, generator reactance must be held to a minimum. A maximum value of three percent subtransient reactance was set for the short-circuit generator, whereas the usual range for power-producing generators is 10 to 25 percent. When the generator is used for tests at 16.5 kv without the transformer, the maximum short-circuit current must be limited by reactors to 105 000 rms symmetrical amperes three phase, or 91 000 amperes single phase.

To obtain the minimum generator reactance, it is necessary to design for the highest possible air gap flux density, and to minimize the permeance (magnetic admittance) of the leakage paths, which include the stator slots, the air gap, the end zones, and in general, a portion of the rotor slots. The stator contribution to permeance was minimized by use of wide and shallow slots, and by judicious use of damping structures in the end zones. Saturation of the flux paths in the iron also serves to reduce permeance. The use of these design parameters tended to reduce the room available for coil bracing, which therefore had to be carefully proportioned to make optimum use of the available material properties.

Superexcitation—Superexcitation can be used with test generators to provide a rapid increase in flux just prior to short circuit, which serves to counteract the initial rapid decay of short-circuit current. Normal excitation is 250 volts, 1200 amperes. Superexcitation is accomplished by applying up to 3000 volts (mid-point grounded) through a water-cooled resistor to give about 85 percent voltage. This resistor is shorted out, causing the flux and internal voltage back of transient reactance to rise faster than the terminal voltage. In seven cycles, the terminal voltage reaches normal and the short circuit is applied. Since internal voltage is high and rising, the natural decrement of the machine is cancelled and current and recovery voltage are maintained. Under normal excitation and maximum output, three-phase current is reduced 15 percent and the single-phase current 9 percent in two cycles after the crest of the first half cycle; with maximum superexcitation the reduction is only 7 percent for three-phase current and 3 percent for single-phase current in two cycles.

Stator—Thermalastic-insulated stator coils are proportioned to obtain equal heating during short circuits in both top and bottom coil sides to reduce relative movement. The conductor dimensions were selected also on the basis that all heat energy generated in them during a maximum

Fig. 3 (Left) The large test generator is driven by a 1750-hp wound rotor motor. Fans are at right.
Fig. 4 (Below) A schematic diagram of one phase of the current limiting reactors.
Fig. 5 (Right) The three single-phase transformers are each rated at 50 000 kva.

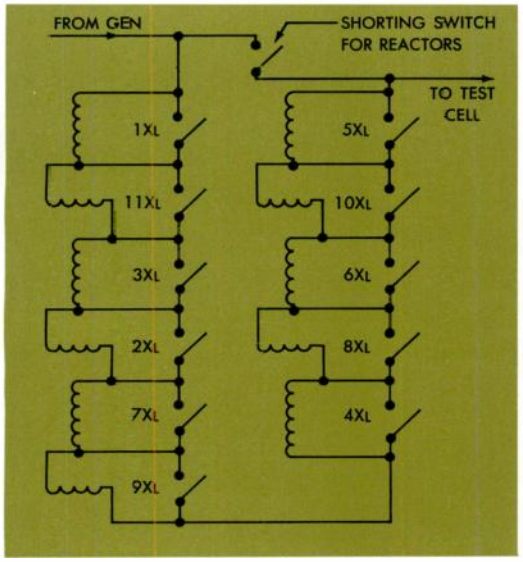

short-circuit duty cycle is stored, to be slowly dissipated during the ensuing rest period. This resulted in shallow coils that are of nearly square cross section; they have little rigidity, and must be carefully supported against the large electromagnetic forces that act on them. The support structure, however, must not prevent their thermal expansion. This dual-purpose support is accomplished by slot wedges in the core portion and end support cones that support the coil ends. The coil end support structures are heavy steel fabricated cones against which the coils are individually supported by use of both solid and pliable insulating materials. Sliding fits and slip layers are used to accommodate thermal expansion.

Another special feature is the spring mounting which consists of many leaf springs along the sides of the stator to reduce shock to the foundation.

Rotor—The generator rotor consists of a single-piece steel alloy forging procured with the usual attention to high quality. It is provided with integrally machined couplings for attachment to the connecting shafts at both ends of the main generator shaft. Slots are cut in the rotor body to accommodate the field winding and slot wedges; additional shallow slots are located in the pole faces to accommodate damper bars. The entire steel surface is grooved to reduce losses and improve heat dissipation.

The rotor supports two windings with widely differing characteristics—the field winding and a damper winding. The former is similar to a conventional field winding, but its insulation is adequate for 1500 volts to ground thus permitting application of 3000 volts (mid-point grounded) for superexcitation. The damper winding consists of the slot wedges, which serve the dual purpose of supporting the field winding and providing damping action, the pole-face damper bars, connecting strips, and end connections. This dual function of the slot wedges requires that they be tight against the field winding, yet free to move axially under thermal expansion. They are therefore made in sections with connecting strips between to provide a continuous current path.

The end connections of the damper winding are provided by nonmagnetic retaining rings in conjunction with low-resistance alloy cylinders in intimate contact with the interior surfaces of the retaining rings. The retaining rings are mounted on the rotor body with heavy shrink fits. They provide the main support for the end windings against centrifugal force. The low-resistance alloy rings are keyed to the shaft to withstand the effects of the short-circuit torques, which result in decelerations as high as 100 g. All current-carrying joints in the damper structure are precisely machined pressure connections with a special surface treatment to reduce wear due to differential thermal expansion. The resulting damper winding is very nearly uniform about the rotor periphery.

Collector and Brush Rigging—A force-ventilated collector of conventional, helically grooved rings is mounted on the shaft end. It and the brush rigging are suitable for the superexcitation voltage. The brushes are retractable, to minimize wear during the relatively long periods when no field current is applied but the generator is at speed. A pneumatic brush-lifting device is employed, and is controlled by an interlock that prevents motion of the brushes if operating air pressure fails.

Switchgear Equipment

The leads from the generator go directly to a segregated phase switchgear structure. This structure includes lightning arresters that protect the generator from overvoltage, the wye-delta switch, the backup breaker, a bypass

breaker, closing switches, and instrument transformers.

Protection of the new testing generator required the design and construction of an entirely new and larger generator breaker. To fulfill this requirement a compressed air circuit breaker rated at 16.5 kv and capable of handling 4560 mva was developed. The breaker has a continuous current rating of 2000 amperes, a momentary rating of 168 000 amperes rms asymmetrical, and a trip time slightly in excess of 5 cycles. The 60-cycle withstand voltage is 50 kv, while the impulse voltage rating is 110 kv. Operating air pressure is 150 psi.

Design considerations required that more current be interrupted than any existing breaker was capable of handling. The breaker also must handle recovery voltage rates that are exceedingly high, as the breaker is located near the generator it is protecting. The backup breaker consists of two essentially conventional compressed-air breaker units in series, mechanically closed and opened by simultaneous control, and with one unit paralleled by a five-ohm resistor in each phase. Contact parting time is adjusted to first insert the resistance and then interrupt the lowered final current. In this way effective control of the most severe rate of rise of recovery voltage is obtained and at the same time, sufficient interrupting capacity is obtained. The complete assembly is 102 inches wide, 114 inches deep, and 125 inches long.

The by-pass breaker maintains normal frequency recovery voltage with much reduced power limits on the breaker on test. A resistor in series with the by-pass breaker permits only a small current to flow in case the test breaker experiences trouble during the heavy power test or fails to withstand normal recovery voltage.

On opening tests, the asymmetries of both single-phase and three-phase currents are controlled by the laboratory closing switches, which close in 12 milliseconds and can be timed to repeat within plus or minus five electrical degrees at any point on the voltage wave.

The closing switches are air-operated single-pole units with three single-pole units and accessories mounted in the switchgear structure above the generator circuit breaker. Each pole unit is controlled individually by its own solenoid-operated pneumatic pilot valve; thus, either independent or simultaneous closing is possible.

Reactor Room and Transformers

For varying the short-circuit test currents in suitably small increments, eleven reactors are used in each phase. A schematic of one phase of the current-limiting reactors is shown in Fig. 4. The maximum impedance with all reactors in series is about 11 ohms per phase. Therefore, the minimum test current at 16.5 kv is a little less than 1000 amperes. The reactors can control the short circuit in $2\frac{1}{2}$ percent steps for single-phase testing, or 5 percent on three phase.

All of the 16.5-kv switches in the reactor room are air-operated and controlled from the control room. A total of 55 air-operated 16.5-kv switches are located in this area. In addition to varying the current-limiting reactance, these switches transfer the test circuits to the 16.5-kv test bus, to the capacitor bank area, or to the primaries of the high-voltage transformers. Furthermore, the transformer primaries may be connected either in parallel or delta by

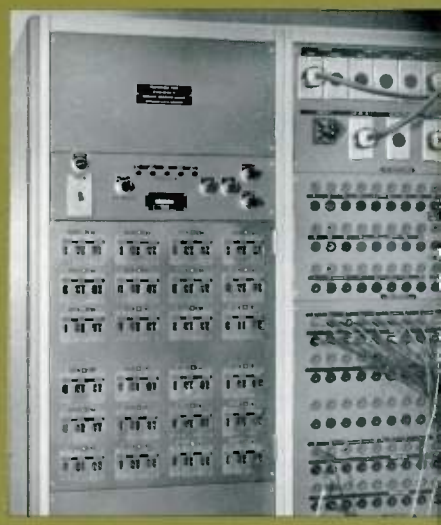

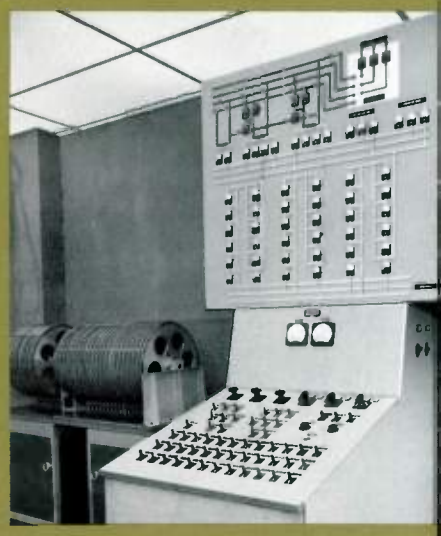

Fig. 6a This control room overlooks all of the test cells. The mai control desk is at far right; the setup panel and current compute are at rear in the photo. The two sequence timers are in the lef center background.

6b) The 24-channel programmable sequence timer.

6c) The rotating drum switch.

remotely controlled switches located in this area and operated from the control room.

The transformers are also of novel design. In addition to being braced to stand the repeated short circuits, they also have inner cooling to give a minimum of insulation space. This was a definite advantage in giving low reactance at a 1300 BIL. The three single-phase transformers, each nominally rated at 50 000 kva with 3.3 percent reactance, are capable mechanically and electrically of delivering 500 000 kva each. The transformers are located under the high-voltage structure, as shown in Fig. 5.

Each of the three step-up transformers has four secondary 22-kv coils, with remotely controlled internal switches for connecting the four coils in series, series parallel, or parallel. These transformers, together with six transformers in the older lab, permit the full 2500-mva single-phase capacity in every step to 132 kv, and also at 220 kv and 264 kv. About 60 percent capacity is available at several other voltages up to 572 kv. For three phase, at transformer voltages, 3200 mva can be obtained at the 22-kv steps up to 88 kv, and at 154 kv. As mentioned previously, the new secondaries are insulated for 1300 volts BIL. All windings are protected against surges by arresters.

Control Room Facilities

The control room overlooks all of the test cells through shatterproof windows. The general arrangement of the instrumentation and control is shown in Fig. 6a. The main control desk, located in front of the viewing windows, contains the control switches and indicating instruments. Above the viewing window are cubicles containing annunciators and bells, which give visible and audible indications of the operation of protective devices and of malfunctioning of vital auxiliaries.

A setup panel and current computer from which the plant operator may check the condition of all the power circuits before initiating a short circuit test is located adjacent to the main control desk. The main power circuits are laid out on this panel and lights indicate the position of all the controls actuating power disconnect switches. The pneumatically operated power switches are located on the setup panel.

One of the most essential pieces of control in the laboratory is the sequence timer. Once everything is set for a test, the timer closes and trips the proper breakers at the proper time; also, it controls the measuring instruments, such as oscillographs, so that records of the essential phenomena are obtained. The sequence switch, or at least some of its contacts, must operate precisely as control of current symmetry is nearly always required. This means that the switch contacts must be adjustable within a few electrical degrees and they must always be consistent in their closing time.

Two types of sequence timers are used in the short-circuit laboratory: A 24-channel programmable timer (Fig. 6b) and a rotating drum switch (Fig. 6c).

The programmable timer consists of a rotating disc with slots spaced so that a lamp (with a suitable optical system) activates a photo cell behind the rotating disc once every six electrical degrees, or 60 times per cycle. The amplified output of the photo cell operates digital counters once the timer has been put in operation. The disc is driven by a miniature synchronous motor, which obtains power from a pilot generator directly connected to the shaft of the main short-circuit generator. When the start switch of the timer is operated, a peaking transformer is employed to delay the start of the counting operation until a predetermined point on the pilot generator voltage wave. This is necessary as the timing must always be started from the same point on the 60-cycle voltage wave.

Dial switches on each channel of the timer can be set for delays from 0 to 35999 pulses, or from 0 to 10 seconds. When the counters total a number of impulses agreeing with the dial setting, the output relays are energized. The output relay contacts control the tripping and closing coils of the power apparatus.

The rotating drum switch, shown on the left side of Fig. 6c is driven by a permanent magnet type synchronous motor (powered by pilot generator) geared to one slow-speed drum with 20 channels and making a revolution in 7½ seconds. It also has one high-speed drum turning at one revolution per second and having eight channels. For controlling the breakers and switches requiring precise timing, a slow-speed drum switch is used in series with one from the high-speed drum, so that the delay in energizing a control circuit can be varied continuously over a range of several seconds in steps of a few electrical degrees.

The final product of a testing laboratory is a collection of data. Therefore, the task of the laboratory is twofold; it must provide the power equipment and circuits required to make tests, and it must make reliable records of the performance of the test piece. The requirements for the equipment needed to protect modern transmission systems are far more severe than they were 25 years ago, so that test facilities and measuring equipment must keep pace with modern requirements. Not too long ago, the magnetic oscillograph was the only instrument required to record the performance of a circuit breaker. Today's instruments must measure many quantities, particularly transient recovery voltages, reliably and accurately. For example, three 12-element magnetic oscillographs are provided, and two rotating-drum, cathode-ray oscillographs can be used to stretch a cycle out to one meter—200 microseconds per centimeter. A delay line has been developed that permits catching any part of the transient recovery voltage record stretched out to one microsecond per centimeter on the electrical sweep, cathode-ray scopes. For current measurements, special current transformers will record any dc transients encountered.

The laboratory has been planned to give not only increased capacity and increased accuracy, but also to provide for more efficient operation. Everything has been done to get more tests per day with a minimum expense. This is important because of the heavy development demands of the immediate future.

REFERENCES
"An Enlarged High Power Switchgear Testing Laboratory," G. L. MacLane, R. C. Van Sickle. IEEE *Transactions* III, No. 63–67.
"A New Three-Million KVA Short Circuit Generator," L. A. Kilgore, E. J. Hill, C. Flick. IEEE *Transactions* III, No. 63–213.
"Switchgear and Control Features of Enlarged High Power Testing Laboratory," W. B. Batten, R. P. Baumgartner, G. W. Champney, W. A. Fish, J. K. Walker, IEEE *Transactions* III, No. 63–56.
"Measurements in a Modern High Power Switchgear Testing Laboratory," D. J. Burns, G. L. MacLane. Presented at IEEE 1963 Midwinter Convention, CP63–69.

Digital Computer Control for the Basic Oxygen Steelmaking Process

E. J. Borrebach
Metals Province Engineering
Industrial Systems
Westinghouse Electric Corporation
Pittsburgh, Pennsylvania

The high productivity of this new process can be increased by digital computer control.

Use of the basic oxygen steelmaking process is growing extremely rapidly all over the world. By 1964 there will be about 84 plants in 23 countries with 75 million ingot tons per year capacity; in 1954 there was only one plant outside Austria, where the process was developed in 1951. This revolution in steelmaking is occurring because of the process' high tonnage capacity, low plant capital and operating costs, simplicity of operation, and ability to produce quality steel. (See *The Basic Oxygen Process*, p. 42.)

High tonnage capacity, the paramount advantage of the process, results mainly from the speed of the operation—a heat of steel can be finished in ¼ to ⅛ the time required for making a heat in an open-hearth furnace. However, this important advantage is not yet fully exploited because control methods are largely empirical. The quantities of furnace charge materials required are determined from graphs or charts and varied in accordance with the furnace operator's experience.

With these control methods, heats are on-temperature at the end of the blow period no more than 60 to 65 percent of the time in this country. When they are off-temperature, the time required for correcting temperature reduces the productivity of the process. (Some Japanese furnaces are said to be brought in on-temperature 70 to 80 percent of the time. However, the Japanese use hot-metal mixers to obtain nearly uniform hot-metal temperature and analysis for a long series of heats. Hot-metal mixers are used in only one basic oxygen furnace installation in this country.)

The frequency of on-temperature heats could be greatly increased by control based on fast accurate solution of mathematical equations that describe the process. The resulting reduction in delays for temperature correction would increase productivity significantly. The equations would be complex, so a computer system is needed to solve them fast enough to keep up with the process. Information obtained by Westinghouse from the construction of a mathematical model of the process, programming of a digital computer to control the model, and testing carried out with actual furnace operating data demonstrates that computer control for a broad range of furnace product can be applied with present instrumentation and present process knowledge.

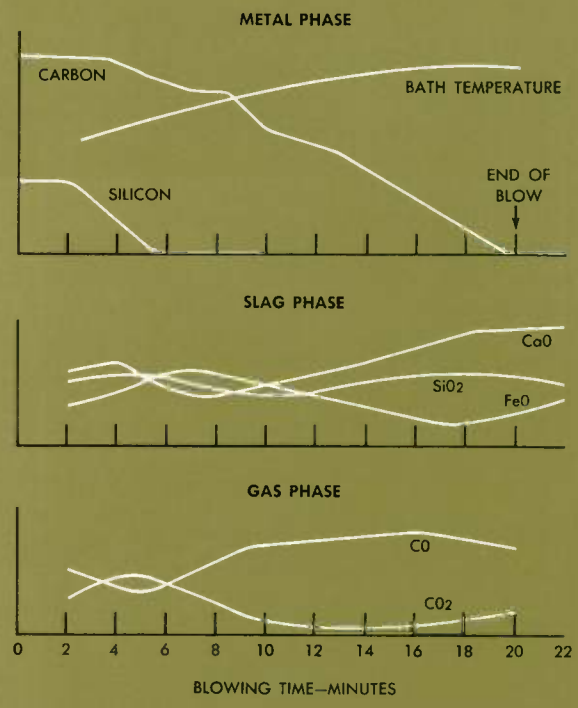

Fig. 1 Variations of the concentrations of several process constituents during the oxygen blow time are illustrated by these graphs. This information was obtained from operation of an actual furnace.

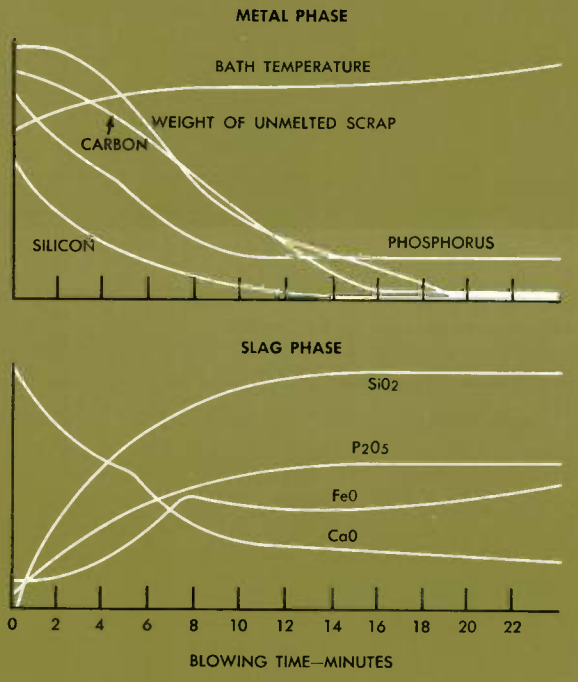

Fig. 2 Operating variables in the simulated basic oxygen process are plotted by the analog computer. The plots agree well with actual operating data, such as that illustrated in Fig. 1.

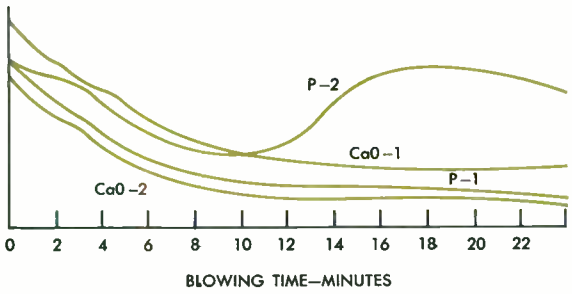

Fig. 3 Different lime (CaO) additions have large effects on the phosphorus (P) content of the steel "produced" by the simulated process. (CaO-2 = 0.80 CaO-1.)

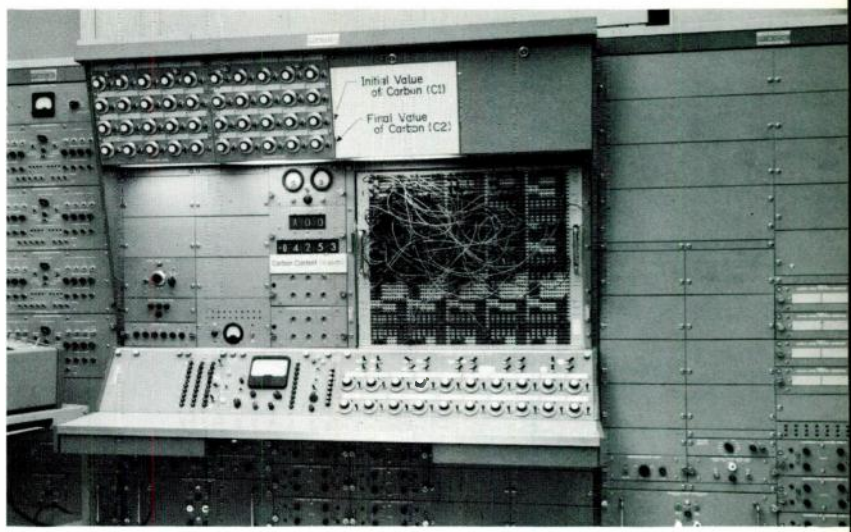

Photo Equations that describe the basic oxygen process are entered into this analog computer with the patchboard. Their solution simulates process operation.

Two basic oxygen installations now have analog computers that solve for the scrap weight required to obtain end-point temperature control. However, these are one-product plants so far as use of the analog computer is concerned. For this one product, the computer solves one equation for one unknown while considering as constant such variables as end-point weight, end-point analysis, lance height, oxygen blowing rate, oxygen blowing time, heat losses, and fume losses.

An analog computer can be useful in such one-product plants and also for helping train furnace operators and showing where present control procedures are inadequate. However, a digital computer, with its flexible programming possibilities, is called for when several different steels are to be produced and when end-point temperature, weight, and analysis must all be controlled. Use of a digital computer also permits inclusion of automatic weighing, programmed control, and data-logging functions in the control system.

The already high productivity of the process should be increased appreciably by application of such a control system. On that premise, Westinghouse has conducted a major program to develop a complete and fully integrated computer control system for the basic oxygen process.

Process Study

Instrumentation for measuring variations in bath temperature and bath analysis during the blow period does not yet exist. Therefore, the process was described through thermal, chemical, material-balance, and mass-transfer equations based on input data and theoretical rates of change. The process will be further described with kinetic equations when in-process data on bath temperature and bath analysis are available. Without this feedback information, however, it is necessary to know how the material concentrations in the metal, slag, and gas phases in the furnace vary with time. The process then can be controlled by preselecting the quantities of charge materials and the blowing cycle values.

The variations of several constituent concentrations with time for the metal phase, the slag phase, and the gas phase of the process are shown in Fig. 1. This information was obtained from a German study of an actual basic oxygen furnace. As shown, the carbon oxidizes relatively slowly until much of the silicon is gone, and the iron oxide in the slag varies throughout the blowing period. (Productivity is partly determined by the amount of iron tied up in the slag at the end of the blow.) The ratio of carbon monoxide to carbon dioxide varies over a wide range. During the latter part of the blowing cycle, however, when this relationship could be useful in determining the end of the blow, the ratio is almost constant.

To interpret these observations, the process was divided into several reaction areas and material-balance and mass-transfer equations covering the various phases were written. A series of equilibrium equations was written to describe the interface reactions. An example of this type of equation, describing reactions in the bulk metal phase, is:

$$d(V_m C)/dt = -K_c' A_m (C - C') - K_c A_s (C - C'').$$

This equation states that the rate at which the concentration of carbon changes with time is proportional to the difference between carbon concentration in the bath C and at the metal-gas interface C' considered over the interface area A_m; it also is proportional to the difference between carbon concentration in the bath C and at the slag-metal interface C'' considered over the area of that interface A_s. The same type of equation applies to silicon, phosphorus, manganese, sulfur, and other constituents.

Similar equations were written for the other process reactions, and an energy balance equation was written to balance the energy inputs from hot metal and oxidizing reactions against the energy used in heating the furnace materials and lost in radiation and convection.

The basic equations were then expanded to take other materials and variables into account and thereby describe the operation of an actual oxygen furnace. These equations, constituting a mathematical model of the process, were entered into an analog computer. Initial and final conditions can be set with control dials on the computer, so solution of the equations simulates process operation.

Several of the process operating variables can be plotted by the computer as functions of time on an X-Y plotter as shown in Fig. 2. Note how quickly silicon is eliminated during the blow, how weight of unmelted scrap varies, and

how iron oxide in the slag changes in a manner similar to the variations shown in Fig. 1. The mathematical model simulates the actual oxygen process with a high degree of accuracy. For example, it has shown that iron oxide content in the slag is a function of lance height during portions of the blowing period, confirming results published by a Russian experimenter. Another example of the model's capability is its reaction to different quantities of lime addition (Fig. 3). Insufficient lime causes high phosphorus content in the metal in the actual process, and the model accurately simulates this effect.

Control Development

The next step in the study was development of a digital computer control to calculate the weights of materials to be charged, oxygen blowing conditions (oxygen rate, lance height, and their variations during the blow), and when to stop the blow to result in the desired end-point analysis, temperature, and weight. This step was based on the premise that if a digital computer can be programmed to run the mathematical model and produce the desired end-point results, it can be programmed in a similar manner to control an actual furnace installation.

Equations describing the interrelationships of the process variables were written and, with these equations, a laboratory type digital computer was programmed. The program enables the digital computer to control the mathematical model (analog computer). The computer is programmed at this time to control end-point temperature, carbon content, and phosphorus content. It is able to control these values within the desired limits over the full range from low- to high-carbon heats.

Data from more than 200 furnace heats were then obtained for testing the digital computer control. From this data and the equations, the end-point values of temperature, weight, and analysis were determined for a number of the heats. The results were good: temperature averaged within 35 degrees F of the actual value, weight within 4000 pounds, and carbon content within 4 points.

Such success with computer control of the mathematical model indicates that an on-line digital computer control system can be applied successfully to the actual process to control end-point analysis, temperature, and weight.

The Prodac computer control system designed for the actual process is diagrammed in Fig. 4. The figure illustrates the high degree of automation in programming and process control that is possible with presently available instrumentation and control devices. A process computer would be worthwhile even without automation—the furnace operator would use the computer to solve for the necessary charge material quantities for each heat but would control computer inputs and process operation himself. However, a complete programmed control system would optimize process productivity and profitability.

The control system illustrated in Fig. 4 will be programmed to schedule each heat on the basis of the number and size of molds required, mold inventory data, and priority assigned to the heat. This information, and also the temperature, analysis, and weight requirements for the heat, will be put into the computer memory with input data cards. The computer also will accept and store the analog and digital inputs received from the weighing, temperature-sensing, and analyzing equipment for use in the necessary computation and control functions.

Computation functions include calculating, for the selected heat and for the desired end-point conditions, the amount of hot metal needed from each torpedo car (hot-metal car), amount of scrap and flux required, lance height, oxygen blowing rate, and oxygen blowing time. The computer will make these determinations on the basis of material weights, temperatures, and analyses and from stored information pertaining to the previous heat (such as lining temperature, time elapsed since the previous heat was tapped, and number of times the lining has been used). On the basis of steel temperature and analysis at the end of the blow period, it will compute the conditions for any reblow or coolant cycle required. Ladle additions required also will be computed on the basis of final steel temperature and analysis.

Control functions are based on the calculations and include rotation of each torpedo car, weighing of the hot

Fig. 4 This diagram illustrates a basic oxygen plant and the computer control system designed to operate the process. Basic information for each heat is entered with an input data card, and the other information required for computation and control is supplied by the stored program and plant instrumentation.

THE BASIC OXYGEN PROCESS

The basic oxygen steelmaking process is carried out in a furnace shaped somewhat like a Bessemer converter (Fig. 4). Steel scrap, molten iron, and fluxing materials are charged, and oxygen is blown through a water-cooled lance onto the top of the charge for 15 to 30 minutes. Oxidation of the charge materials, including some of the iron, raises the temperature of the bath. Carbon is lost through the furnace mouth as carbon monoxide and carbon dioxide, and the flux removes other unwanted materials by combining with their oxides to form a slag.

If bath temperature is not correct for furnace tapping at the end of the blow, the operator initiates another oxygen blow (to increase temperature) or adds scrap or lime (to decrease temperature). He may also have a sample of the steel analyzed and, if necessary, initiate another oxygen blow or add materials to correct the composition. When temperature and composition are correct, the operator tilts the furnace to pour the heat into a teeming ladle. Various materials may be added in the ladle to produce the final analysis desired, and the heat is teemed into ingot molds.

A typical oxygen furnace plant has two or three furnaces and the necessary storage and conveying systems for scrap, fluxes, and ladle additives. Special cars operating on rail tracks bring in hot metal from the blast furnace. Other cars handle the slag pots, teeming ladle, and ingot molds.

Most of the world's steel is presently produced by the open-hearth process, but the rate of growth of the oxygen process indicates that all new steelmaking plants will be of this type. The higher tonnage capacity of the basic oxygen process is the main reason for its growing popularity. Tonnage capacity is higher because the process is much faster—a heat of steel can be produced in an hour or less, compared with several hours for the open-hearth process. This higher productivity results in lower capital and operating costs. At the same time, the process produces steels comparable in quality and variety to those produced by the open-hearth process.

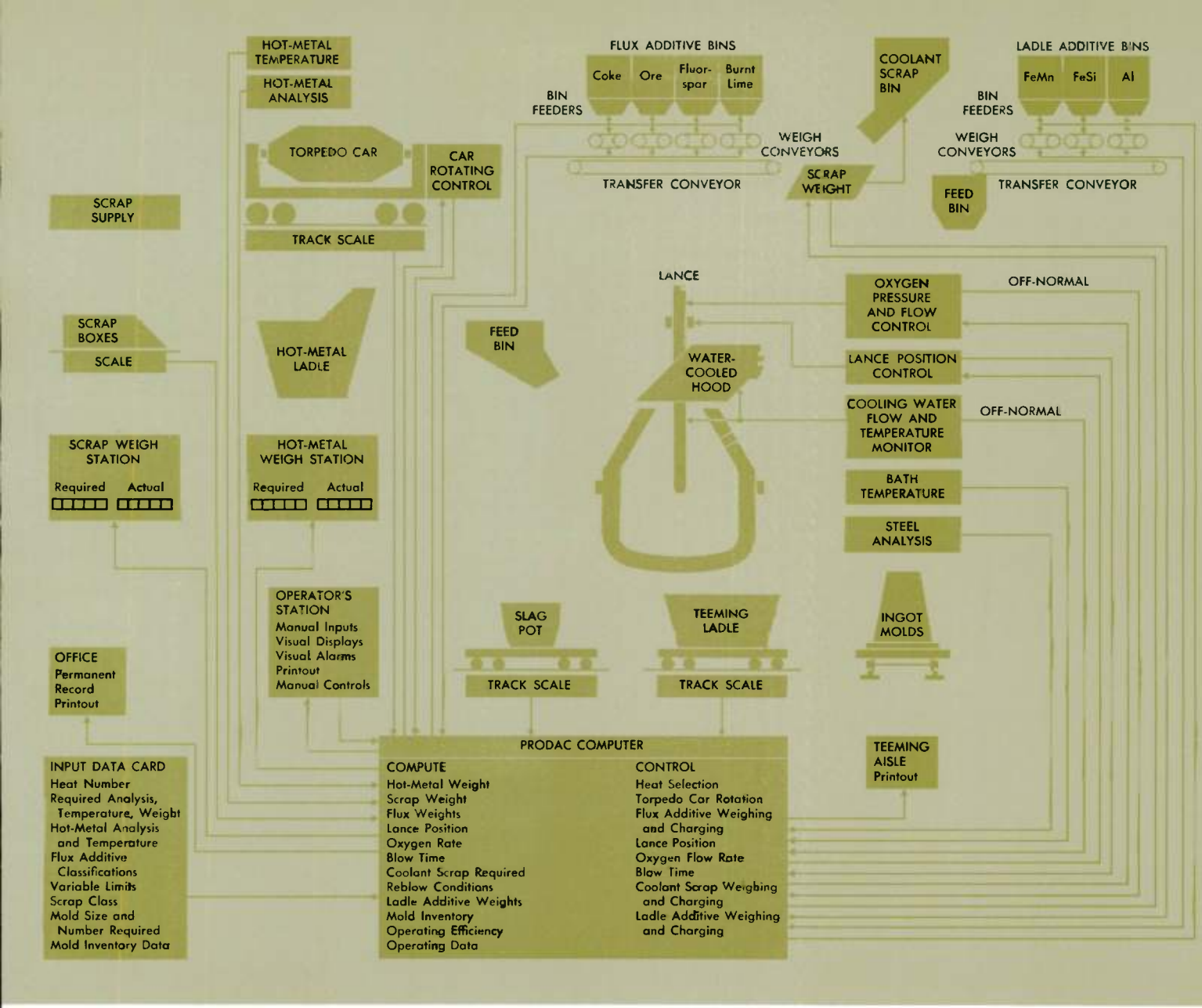

metal poured, weighing and charging of the flux additives, positioning of the lance, starting and stopping of the oxygen blow, and control of oxygen blowing rate. The system also will control similar functions for reblow and coolant cycles and will control weighing and charging of the ladle additions.

Further, the control system will monitor for off-normal conditions in cooling water temperature and pressure and in oxygen flow and pressure. It will calculate quality-control, operating, and production data at the end of each heat. Printout devices at the main operator's control desk and in the superintendent's office will log all pertinent process information, including input-card data, calculated values, measured input values, off-normal conditions, and quality-control, operating, and production data. Finally, the computer will revise its own program continuously on the basis of operating experience. This program updating will take into consideration instrumentation changes (as when more accurate measuring equipment is applied) and minor process revisions that, through experience, are found to improve control or productivity.

Conclusion

A digital computer control system that provides data logging, automatic weighing, programmed control, and end-point control can reduce production costs by optimizing the oxygen blowing conditions and the quantities of charge materials used. It will increase yield by controlling lance height and blow rate to assure low iron content in the slag, and it will improve quality control by controlling analysis in the vessel as well as in the ladle.

Efficiency will be increased by eliminating off-analysis heats and by producing heats of the desired weight. Productivity will be increased by minimizing time delays from off-temperature or off-analysis heats. After a considerable amount of control experience has been accumulated, the need for a preliminary analysis part way through a high-carbon heat could be eliminated.

SOLIDIFICATION . . . The Freezing of Crystals from Liquids

Much of our modern technology depends on new developments in materials—materials that are extremely pure in a single element, or have precise amounts of alloying elements added in a controlled fashion. Freezing—the formation of a crystalline phase from a liquid or melt—is a critical step in building these new materials. Use of the freezing process ranges from large castings to the preparation of minute inhomogeneities in tiny solid-state devices.

Controlled Freezing

The change from a liquid to a solid is driven by the extraction of heat from the liquid. This phase transformation can be separated into two parts: the initial formation of crystals, and the growth of these initial nuclei by accumulation of atoms from the melt. Initial nucleation occurs when a liquid is *undercooled* below the melting temperature by some critical amount, δT_c. Depending upon the material and environmental conditions, δT_c can range from hundredths of a degree to over 100 degrees.

Solute Manipulation—Most liquids are solutions of several elements: a major element (the *solvent*), and alloying or impurity elements (*solutes*). One of the major uses of the freezing process arises from the fact that as a liquid is frozen progressively in a controlled fashion, the concentration of solute in the frozen phase can be made to differ from the concentration of solute in the liquid phase.

The property of the solute that allows its manipulation during freezing is that the atom fractions of solute in the solid and liquid phases at equilibrium are different. This difference is defined by the equilibrium partition coefficient, k_o, the ratio of the solute concentration in the freezing solid, C_s, to the solute concentration in the liquid, C_o: $k_o = C_s/C_o$.

Solutes having $k_o > 1$ raise the melting point of the solvent; solutes with $k_o < 1$ lower the melting point of the solvent, as illustrated in Fig. 1. In either case, freezing can begin when liquid temperature reaches T_o, the temperature at which a solid of concentration k_oC_o is formed.

The equilibrium partition coefficient (k_o) is rarely achieved in a real freezing process, although it may be approached closely. Since $k_o < 1$ is the much more common situation, only this condition will be considered here. The equilibrium conditions for a solid-liquid interface with $k_o < 1$ are shown in Fig. 2a. However, this condition cannot be achieved with a moving interface unless the rate of freezing is very small or forced mixing of the liquid is great; therefore, since solute is rejected by the freezing solid, it accumulates at the advancing solid-liquid interface as shown in Fig. 2b. Here, the solute concentration freezing out in the solid is increased over the equilibrium conditions. But since the equilibrium partition coefficient (k_o) must exist at the interface ($C_s/C_L(0) = k_o$), the effective partition coefficient (k) changes from k_o. If freezing takes place at a fast rate, k approaches 1, and C_s approaches C_o.

Two basic procedures are used for careful freezing of a solution: *Normal freezing*, where a solution is frozen progressively from one end of a melt, and *zone melting*, where a molten portion is moved through the solid so that both melting and freezing are performed progressively.

Normal Freezing

This procedure, generally used for preparing single crystals, can be imagined as proceeding along a cylinder from one end. Since the rejected solute accumulates in the liquid as freezing proceeds, the increasing liquid concentration produces an increase in the concentration freezing out, causing an end-to-end segregation.

For constant conditions during freezing, four distinctly different types of segregation curves can result from normal freezing, as illustrated in Fig. 3: (a) Freezing is so slow that diffusion in the liquid and solid eliminates all concentration gradients thus maintaining equilibrium at all times. This case, called *equilibrium freezing*, leads to no

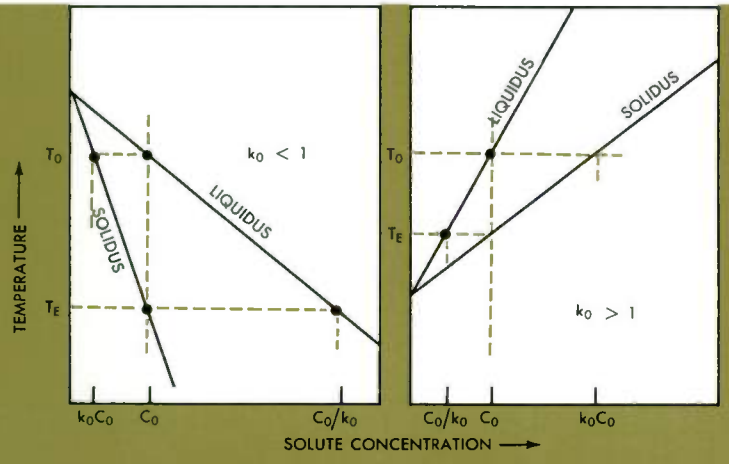

Fig. 1 Portions of phase diagrams for cases where the solutes either lower ($k_o < 1$) or raise ($k_o > 1$) the melting point of the alloy relative to the pure solvent. Freezing will start at temperature T_o.

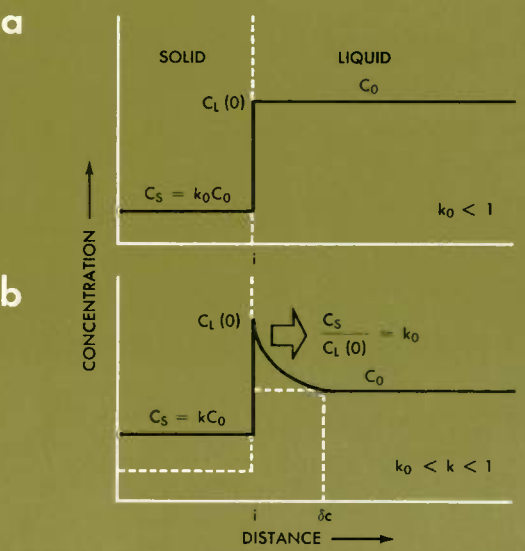

Fig. 2 For a solid liquid interface when $k_o < 1$, equilibrium conditions are shown for (a) complete mixing ($k = k_o$) and (b) partial mixing ($k_o < k < 1$).

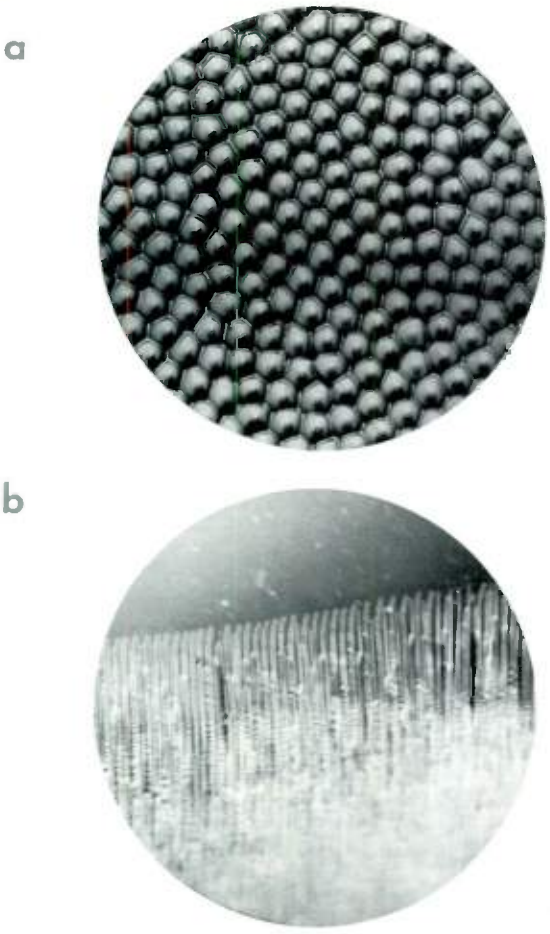

Photo A Photomicrograph of cellular interface morphology in a lead (Pb) crystal with 0.0005 percent (by weight) silver (Ag) solute. The cell borders are high concentrations of solute (100X).

Photo B Dendritic growth in water (10X).

segregation and is never realized in practice because diffusion rates in the solid are too slow. (b) Freezing is slow enough for mixing to erase all concentration gradients in the liquid but fast enough so that diffusion rates in the solid are negligible. This case, called *complete mixing*, leads to the maximum possible overall segregation and may be closely approached in practice. (c) Freezing is rapid enough that only liquid diffusion affects the solute distribution at the interface. This case, called *no mixing*, leads to only slight segregation and is often realized in practice. (d) Freezing and liquid mixing are such that the solute distribution is affected both by diffusion and convection. This case, called *partial mixing*, leads to intermediate segregation and is generally realized in practice.

During buildup of the steady-state solute distribution in the liquid, an *initial transient* distribution is developed in the solid having a form similar to curves (c) or (d).

Increasing or decreasing the freezing rate during freezing can produce an *intermediate transient* distribution, producing bands of higher or lower solute concentration.

As the solid-liquid interface approaches the end of the specimen, the solute concentration in the melt increases, producing a *terminal transient* rise in concentration.

Zone Melting

This procedure, illustrated in Fig. 4a, has made the freezing process extremely useful and versatile and offers certain practical advantages in solute control over normal freezing methods. Some of the process variables are zone length, initial distribution of solute in the charge, mixing conditions, and zone travel rate. By maintaining all of these parameters constant throughout a zone passage, a variety of different solute distributions will result in the solid for different values of k_o (Fig. 4b). If the starting conditions are changed during zone passage, an almost limitless array of solute distributions can be produced.

Zone melting of a uniform rod results in an initial and a final transient where solid concentration is considerably different from the rest of the rod. An improvement in uniformity can be made by passing the zone in the reverse

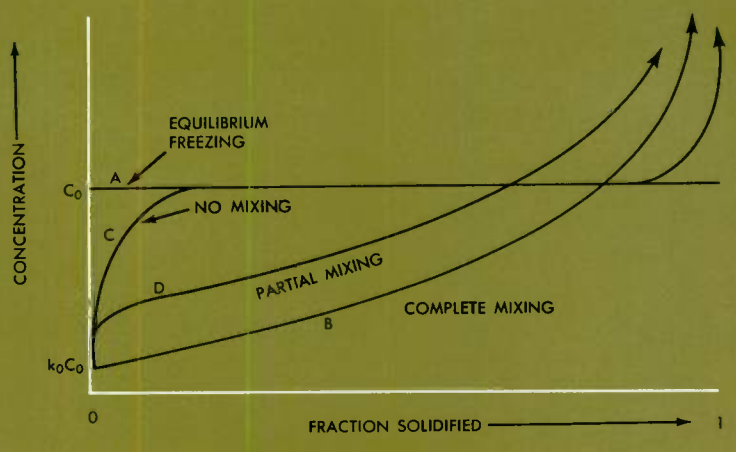

Fig. 3 These solute distributions in a solid bar result from freezing a liquid of initial concentration C_o for the cases: (a) equilibrium freezing, (b) complete mixing, (c) no mixing, and (d) partial mixing.

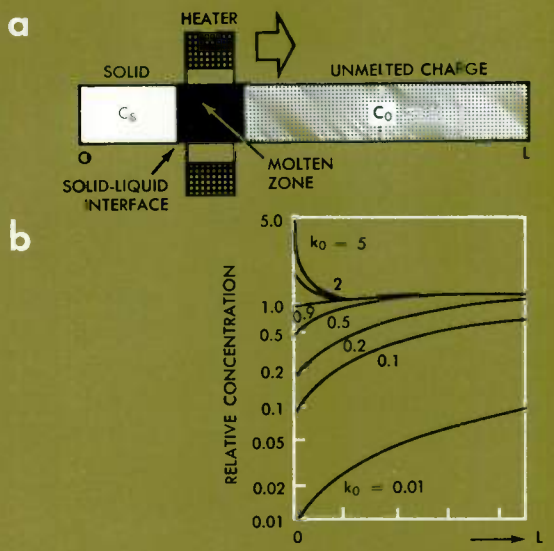

Fig. 4 (a) Schematic illustration of zone melting; (b) relative solute concentration is shown for single-pass zone melting for several values of k_o.

direction. After many passes in the same direction, the solute distribution in the ingot reaches a steady state which represents the maximum attainable separation for the starting conditions.

Solid-Liquid Interface Morphology

A second major function of controlled freezing is to control grain structure during solidification. The interface morphology (microscopic shape of interface during growth) plays a major part in controlling grain structure.

The growth structure of the advancing solid-liquid interface can assume many forms. *Cell formation* (Photo A) is a very important form of interface morphology. Another is *dendritic growth* (Photo B), a special case of cell formation. The particular morphology that an interface will exhibit depends upon such variables as temperature distribution, solute distribution, and the atomic kinetics of the freezing process. Many different interface morphologies may be

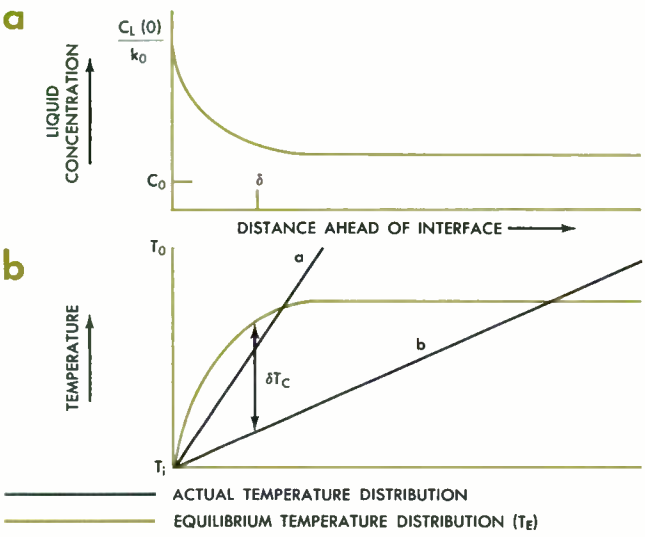

Fig. 5 A zone of constitutional supercooling in the liquid results from solute buildup ahead of the advancing interface.

Fig. 6 Schematic illustration showing the temperatures involved in the dendritic growth process with a negative temperature gradient at the interface.

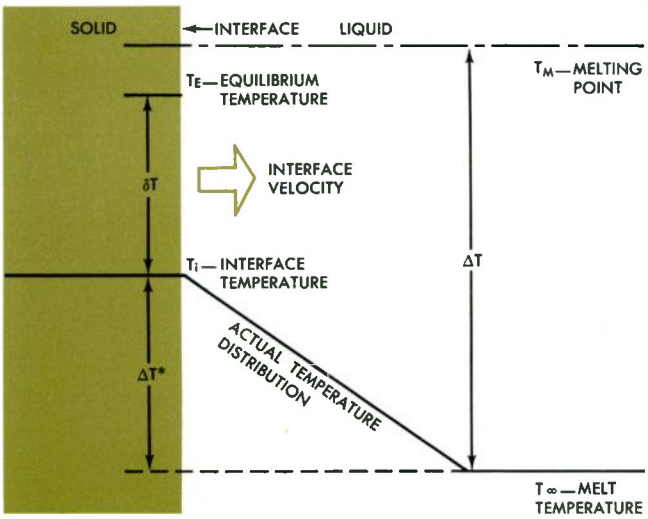

able to satisfy these restraints; however, one form will be able to respond most rapidly to the thermodynamic driving force, and will therefore dominate and overgrow all others. The consequences of interface morphology arise as a result of the particular distribution of chemical and physical imperfection introduced into the crystal structure.

Cell Formation—This form of substructure, shown in Photo A for a Pb (lead) crystal, is produced by the formation of a zone of *constitutionally supercooled* liquid ahead of the advancing interface. The condition results from solute buildup ahead of the freezing interface. A graphical picture of the situation is shown in Fig. 5. The upper curve (*A*) is the typical solute distribution in front of the interface. Referring back to Fig. 1, the equilibrium temperature of a liquid (*Liquidus*) varies with concentration; therefore, the corresponding equilibrium temperature for the melt in front of the interface is shown by the lower curve (*B*). *Actual* temperature distribution in front of the interface may be different from the equilibrium temperature; the slope of actual temperature distribution is dependent upon the rate of heat flow from the liquid to solid. When actual temperature falls *below* equilibrium temperature, the liquid is constitutionally supercooled.

When the amount of supercooling is relatively small, as shown by curve *a* (Fig. 5), the interface degenerates into a cellular form. This produces a cell structure within the crystal, as shown in Photo A. The cell boundaries are high concentrations of solute, which can range from 5 to 10 000 times the concentration of the cell itself.

If the amount of supercooling exceeds the critical value (δT_c) as shown by curve *b*, new crystals will nucleate ahead of the advancing interface, producing a polycrystalline aggregate (grain structure).

Dendritic Growth—Dendritic growth is a specialized form of cell morphology, where cell growth resembles a tree-like structure, which may be either branched or unbranched (Photo B). In a pure melt, dendritic growth can develop into the predominant morphology only if the liquid temperature gradient is negative at the interface. This requires that the liquid be supercooled by some amount (ΔT) below the melting temperature. For alloy liquids it is possible to develop the dendritic morphology with a positive temperature gradient in the liquid provided the solute distribution is such that sufficient constitutional supercooling be developed at the interface. Conditions in front of the interface must fall *between* curves *a* and *b* in Fig. 5.

The important temperatures involved in the dendrite growth process with a negative temperature gradient at the interface are shown in Fig. 6. Temperature difference, δT, controls the rate of atomic deposition onto the solid; temperature difference, ΔT^*, controls the rate of heat flow away from the tip of the dendrite, and thus controls the macroscopic freezing rate. For dendritic growth to occur in a stable fashion, the interface temperature, T_i, must be such that the atomic deposition rate is equal to the macroscopic freezing rate.

The foregoing has been an extremely brief resume of the solidification process. Scientists are presently doing much investigation in this area, and much has yet to be learned. The great need for a more fundamental understanding of crystal growth mechanisms, morphologies, and techniques has resulted in the recent formation of a Crystallogenic Section in the Metallurgy Department of the Westinghouse Research Laboratories under the leadership of Dr. W. A. Tiller. The assignment given this section is to advance the science and develop the technology for preparing materials with specific states of aggregation of both chemical and physical defects.

Technology in Progress

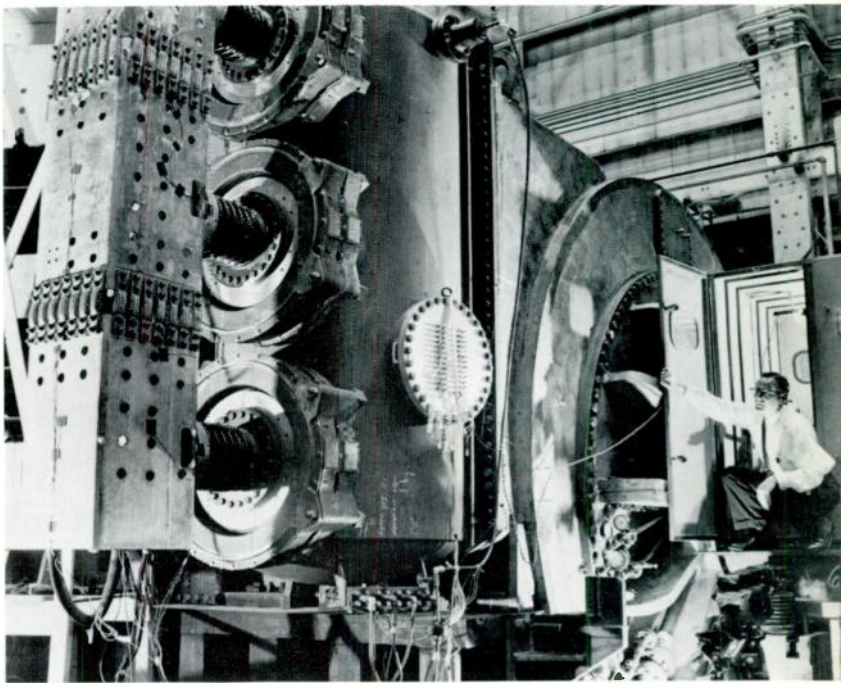

An inner-cooled single-shaft generator rated at 460 000 kva, 19 kv, at 45 pounds hydrogen gas pressure is shown at right being tested before shipment. The outdoor generator has a power capability of 506 000 kva at 60 pounds pressure, and it probably is the world's largest single-shaft generator. The tests demonstrated the feasibility of building inner-cooled single-shaft generators in still larger ratings.

The unit was shipped recently by the Westinghouse Large Rotating Apparatus Division to the Texas Electric Service Company for service at the Handley Steam Electric Station, Fort Worth. It will be driven by a 3600-rpm tandem-compound steam turbine. One unusual feature of the generator is the arrangement of main lead terminal bushings, which protrude from the side of the frame to permit close coupling with the main power transformer.

Conducted Radio Interference Measured on EHV Lines

An accurate technique for measuring conducted radio interference on extra-high-voltage transmission lines has been developed at the Westinghouse Research Laboratories. Verifying measurements have been made on the 345-kv lines of the American Electric Power System in Indiana and on its 750-kv test lines at Apple Grove, West Virginia, using bare-hand live-line methods. The technique was developed in a study of conducted electromagnetic interference made for the Department of the Navy, Bureau of Yards and Docks.

A high-voltage clamp-on current probe designed for the purpose has blocks of ferrite as a high-resistance magnetic medium between the high-voltage conductors and a standard radio noise meter.

A man with the probe and meter is lifted to the high-voltage lines in a metal cage attached to an insulated boom. The cage is electrically connected to the high-voltage conductor to bring the cage to line potential. The man connects the probe to the meter with a coaxial cable, clamps it over the conductor, and takes readings. ■ ■ ■

Calorimeter Measures Light Energy

Conventional techniques for measuring the energy in a beam of light use calorimeters that absorb the beam energy in a small quantity of liquid or a small piece of solid material. The resulting temperature rise is then measured. A basic problem with these calorimeters is that the temperature has to be equalized before the heat rise is measured. This requires stirring (in a liquid) or waiting for equal heat distribution (in a solid). In either case, some heat is lost before equal heat distribution is achieved, and this introduces an error in determining the total energy absorbed.

The problem is especially acute when attempting to measure the energy in the beam from a pulsed laser, for the light pulse is very short—perhaps 0.0005 second. To solve this problem, a calorimeter that measures energy much more directly has been developed at the Westinghouse Electronics Division.

The sensing element of the "rat's nest calorimeter" is a mass of fine insulated copper wire (about 1000 feet of it) packed loosely and randomly into a glass container silvered on the inside to prevent escape of light. The wire is connected into a bridge circuit containing a galvanometer. When a laser beam is fired into the glass container, the heat generated changes the electrical resistance of the wire. This change in resistance appears as a deflection of the galvanometer needle. A permanent record of readings can be made with a cathode-ray oscillograph.

Although the device was developed to measure energy in the beam from a pulsed laser, it is also useful for measuring visible and infrared radiation from any source. The unit is simple and rugged, so it is well adapted for general measurements. The calorimeter is being manufactured by the Electronic Tube Division. ■ ■ ■

Functional Electronic Blocks Increase in Variety

Acceptance of functional electronic blocks by systems designers depends to a large extent on availability of blocks in the variety required to solve systems problems. Many types of blocks are now supplied by Westinghouse, and this variety permits diverse equipment designs.

Functional electronic blocks are only about the size of a match head, yet each performs the work of several electronic components such as transistors, diodes, resistors, and capacitors. Besides the advantage of small size, the blocks can be mass produced, and this should lead to substantial cost savings over conventional circuits. A number of prototype systems and subsystems have been built from the blocks and operated to verify reliable performance.

This motor and gear unit accelerates and brakes rapid-transit cars, yet is small enough to be mounted on a car truck.

An iron bar floating inside the coil of the new superconducting magnet supports this young lady with the greatest of ease. The magnet is not connected to a source of power because, once started, the energizing current continues to flow through the coil at full strength as long as the coil is kept cold by its bath of liquid helium.

Two series of standard blocks are now available from stock at the Westinghouse Molecular Electronics Division. Six linear devices make up one series, and three digital devices the other.

The linear blocks perform a wide variety of communications functions and are so compatible with each other that they can be used as the principal components of complex systems such as radio receivers. Four of the six devices are commercially available for the first time. They are a radio-frequency amplifier, a low-level audio amplifier, a video amplifier, and a wide-band audio amplifier. Previously available, but now improved, are an oscillator-mixer and an intermediate-frequency amplifier.

The digital blocks use the basic NAND structure and can be interconnected to provide all of the digital functions. The series includes two completely new devices—a single-NAND gate and a set-reset flipflop. An improved double-NAND gate completes the series.

In addition to the two series of standard blocks, Westinghouse supplies other blocks to order. ■ ■ ■

Compact Traction Power-Drive System

A new traction power-drive system is small enough to be mounted in the standard inside bearing trucks of most rapid-transit cars. Introduced by the Westinghouse Rectifier and Traction Division, the Tracpak system is designed to electrically accelerate and dynamically brake rapid-transit cars. The unit consists of a high-speed dc traction motor, currently available in ratings to 150 horsepower, combined with parallel double-reduction gearing.

The motor side of the Tracpak system is supported from the truck frame by a resilient vertical hanger that absorbs gravity and torque-reaction forces but permits free axle motion. The axle side is supported by a large double-disc resilient coupling mounted in the truck axle. This axle coupling acts as a two-point support to absorb any twisting motion in the power unit. A horizontal stabilizer suppresses axle-induced vibrations and lateral shock forces.

The self-ventilated motor has four-circuit armature windings, cross connections, and commutators designed to provide maximum commutating capacity for dynamic braking. The class F Epomica insulation and epoxy pressure impregnation resist water and solvents.

The vertical support hanger and side stabilizer are bolted into place during truck assembly. The preassembled resilient axle coupling is pressed onto the axle, and the drive unit is then bolted to this coupling. ■ ■ ■

Superconducting Magnet Produces High Field in Air

A second-generation superconducting magnet produces its magnetic field outside the liquid helium that cools the solenoid. Thus, the intense field can be used in a variety of experiments at any temperature and in any atmosphere. The field of earlier superconducting magnets was available only at —452 degrees F and in a restricted liquid environment.

The new magnet was developed by scientists at the Westinghouse Research Laboratories. It facilitates experimentation that was difficult or impossible with previous superconducting magnets. For example, plasmas can now be passed through a superconducting field to study the reactions found in magnetohydrodynamic generators and electric space propulsion systems; the effects of intense magnetic fields on living tissue can be observed; chemical reactions can be studied under intense magnetism; and the magnetic field can be put to various pulling tasks.

The innovations that made the new magnet possible are development of a high-field solenoid with a sizeable inside diameter and design and construction of a helium container (Dewar) that keeps the coil immersed in liquid helium but locates the magnetic field outside the Dewar.

PRODUCTS FOR INDUSTRY

ADJUSTABLE DC ARC POWER SOURCES meet the requirements of short-arc lamps used for heat generation in solar simulators. They cover the current-voltage requirements of all commercially available mercury-xenon and xenon short-arc lamps. This assures maximum operating efficiency, long lamp life, and precise temperature control. Full-wave silicon rectification is used, with secondary current output adjusted by an electrically reversible gearmotor that operates a moving-core reactor. Adjustments can be made either at the power supply or at a remote location.
Westinghouse Westing-Arc Division, Buffalo, N. Y.

NEW 400-CYCLE COMPRESSOR DRIVE AND FAN MOTORS operate at temperatures from —65 degrees to 200 degrees F. They can endure more than 600 pounds per square inch internal pressure without leaking. Both Refrigerant 12 and Refrigerant 22 can be used with the compressor motors. Compressor motor ratings range from 26 horsepower to 5 horsepower on the same size frame. Fan motors are rated 2.5 horsepower, with speeds from 3600 to 24 000 rpm.
Westinghouse Aerospace Electrical Division, P. O. Box 989, Lima, Ohio.

MINIATURE CURRENT TRANSFORMER is made in both 200- and 400-ampere ratings, 600 volts. The EMW indoor-outdoor instrument transformer has 10-kv basic insulation level and is rated 0.3 ASA accuracy class.
Westinghouse Electric Corporation, P. O. Box 2099, Pittsburgh 30, Pa.

VACUUM GAUGE measures pressures as low as 10^{-9} millimeters of mercury by the ionization principle. The type WL-8057 gauge is five inches long and about two inches in diameter. Its two separate tungsten filaments can be operated singly, in series, or in parallel.
Westinghouse Electronic Tube Division, P. O. Box 284, Elmira, N. Y.

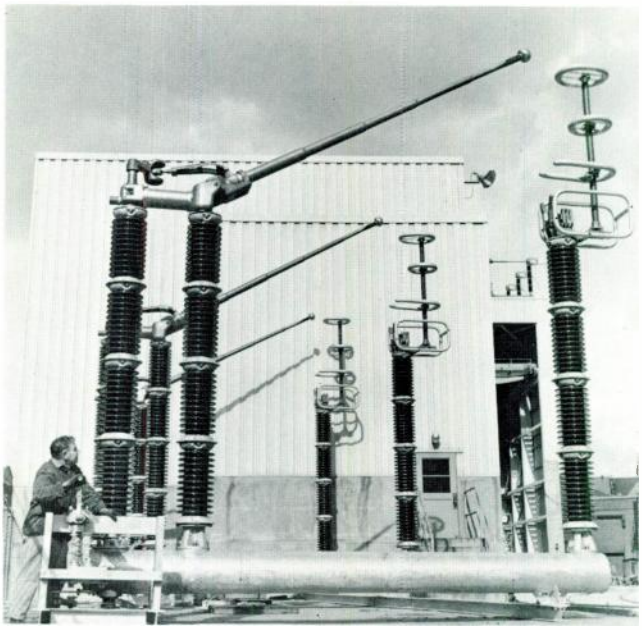

This three-pole disconnect switch serves extra-high-voltage systems.

The Dewar is annular in cross section, with an open space one inch in inside diameter running up through its center. The solenoid's inside diameter is two inches, and it surrounds the open space when in place in the Dewar. When the solenoid is immersed in liquid helium and energized with electric current, it produces a magnetic field of 30 000 gauss in the central working space.

The solenoid is a wire coil about four inches long, four inches in diameter, and five pounds in weight. It is wound from a continuous strand of superconducting niobium-zirconium wire about 15 000 feet long and 0.010 inch thick. A conventional electromagnet supplying the same magnetic field in the same working area would weigh several tons and would require a continuous power supply of about 25 000 watts. ■ ■ ■

Extra-High-Voltage Disconnect Switch

A three-pole vertical-break disconnect switch rated 1550-kv basic insulation level (BIL) now serves 500-kv extra-high-voltage systems. The Westinghouse Type V-2 disconnect switch carries 2000 amperes continuously with a maximum temperature rise of 27 degrees C. Momentary current rating is 80 000 amperes, and four-second rating is 50 000 amperes.

Hinged parts, on the live side, have enclosed blade counterbalance mechanisms, enclosed pole unit stops, and completely enclosed solid bridging construction to transfer current from the hinge to the pivoting blade. A 10-inch sphere at the tip of the blade controls corona when the switch is open. Zirconium copper is used at the break end, and the jaws have silver inserts on the contact surfaces.

One person can open and close a single-pole unit with a hand lever. For ganged three-pole operation, either a handcrank or a motor mechanism with an 8-to-1 gear ratio is used.

The SCOTT-R Development Program

The supercritical pressure once-through tube reactor may be the answer to the need for a nuclear plant to supply high-pressure and high-temperature steam for the turbine generators of the 1970's.

J. H. Wright
Manager, Advanced Reactor Systems
Atomic Power Division
Westinghouse Electric Corporation
Pittsburgh, Pennsylvania

The trend to ever-larger generating plants with advanced steam conditions has several implications in the nuclear field. These trends have encouraged rapid growth of unit sizes; this growth in unit size and typical optimum steam conditions for various unit sizes are shown in Figs. 1 and 2. The information in these charts indicates that large plants, using steam conditions near those used in fossil fuel-fired plants, may be helpful in achieving competitive nuclear power in the 1970's. Specifically, plants should be developed to provide: Six to eight million pounds per hour of steam at supercritical pressures, with provisions for single or double reheat, at an overall cost competitive with conventional plants using fuel at 20 to 25 cents per million Btu.

These steam requirements are above and beyond anything previously contemplated in a reactor system. Water reactors currently can be designed to produce four to five million pounds per hour of saturated steam, but these will fall far short of the objective considerations of the advanced steam conditions that are considered optimum for the ultra-large sizes. If the development program in progress continues according to plan, a reactor plant to meet the necessary requirements should be feasible in the 1970's.

The trend to larger unit sizes will work to the economic advantage of nuclear plants because the differential capital cost burden due to the extra safety measures diminishes with increasing plant size, while the fuel costs from high-efficiency nuclear plants may be appreciably lower than conventional fuel costs. One contributing factor to the lower nuclear fuel costs is the fact that nuclear systems developing the same steam conditions as a fossil-fired boiler will have 8 to 10 percent lower heat rate because there are no flue gas heat losses.

The SCOTT-R Program

A concept which embodies these advantages is the supercritical once-through tube reactor (SCOTT-R), which is

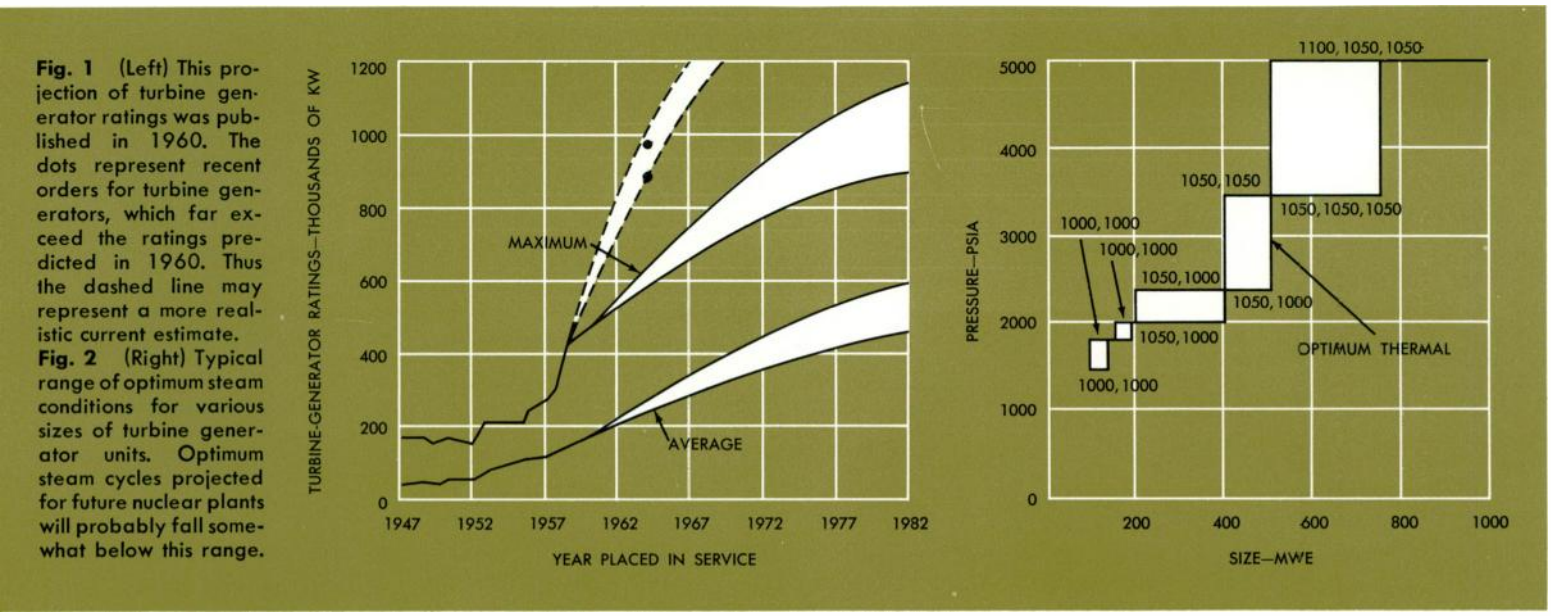

Fig. 1 (Left) This projection of turbine generator ratings was published in 1960. The dots represent recent orders for turbine generators, which far exceed the ratings predicted in 1960. Thus the dashed line may represent a more realistic current estimate.

Fig. 2 (Right) Typical range of optimum steam conditions for various sizes of turbine generator units. Optimum steam cycles projected for future nuclear plants will probably fall somewhat below this range.

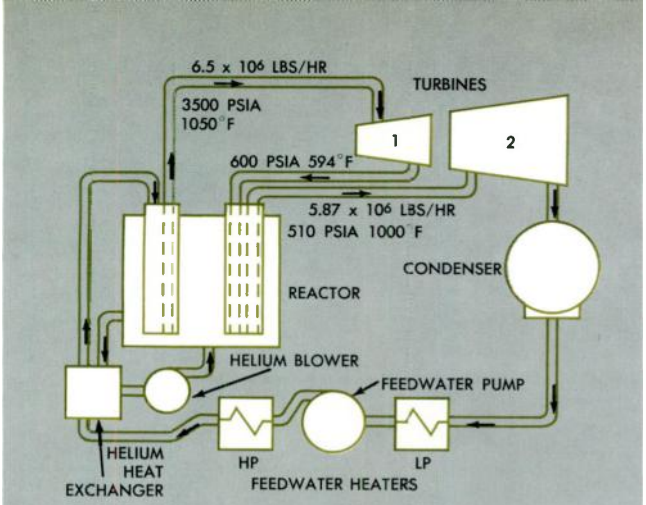

Fig. 3 A schematic diagram of the 1000-mwe SCOTT-R.

currently under development by Westinghouse for the Atomic Energy Commission. A schematic diagram of this system is shown in Fig. 3, and typical parameters for this concept in Table I.

The SCOTT-R size limitation is not dependent upon the feasibility of a single large component, but rather rests with the ability to interconnect and control a number of pressure tubes within a single graphite-moderator mass. This system permits once-through heat transfer, which eliminates recirculation pumps, piping and steam drums; provides on-power control of operation variables; and provides nuclear stability through graphite moderation.

The advanced steam conditions of the SCOTT-R system fit into the steam-turbine trends, noted earlier, to higher temperature and pressures with larger sizes. The SCOTT-R turbine cycle achieves overall net plant efficiency of 43.7 percent and requires a flow of 6½ million pounds of supercritical steam and a single reheat to produce 1000 mw electrical. This net heat rate of 7800 Btu per kwhr is lower than that of a conventional plant with the same steam conditions because there are no heat losses resulting from the boiler flue gas.

Table I SCOTT-R PARAMETERS

System	Direct cycle once-through
Plant size potential	1000 mwe and larger
Steam cycle	3500/1050 F/1000 F
Net plant efficiency	43–44 percent
Specific power, kwt/kg U	15–25
Avg core power density, kwt/ft³	150–250
Typical enrichment, % U_{235}	2.8

Table II COMPARISON OF POWER COSTS FOR 1975 OPERATION

	Conventional	SCOTT-R
Capital Cost,[a] $/Kw	100–110	115–125
Power Costs:		
Capital, 80% P.F. and 14% Annual Charge	2.00–2.20	2.30–2.50
Fuel	2.00[b]	1.15–1.25
Operation and Maintenance	0.30	0.35[c]
Total	4.30–4.50	3.80–4.10

[a] Includes land, interest during construction.
[b] Fuel costs based on 25¢ per million Btu and heat rate of 8000 Btu/kwh.
[c] Includes nuclear liability and property insurance.

The conceptual design of SCOTT-R incorporates about 650 pressure tubes to provide the supercritical and reheat flow channels. Within each of the supercritical pressure tubes and in direct contact with the coolant is a fuel assembly consisting of slightly enriched uranium dioxide clad with stainless steel and fabricated into concentric annular rings. The reheat pressure tubes contain slightly enriched rods clad with stainless steel. The hottest spot on the fuel clad is in the range of 1200 to 1300 degrees F. The 6½ million pounds of steam enters the turbine at 3500 psi and 1050 degrees F.

The steam turbine is a cross-compound 3600/3600-rpm machine having a double-flow, high-pressure front end and a double-flow intermediate section, and four double-flow 28-inch exhausts. This turbine design allows for best use of the nuclear steam source while retaining design characteristics that provide for minimum power conversion costs.

The SCOTT-R reference design can be installed in a relatively small vapor container. A total height of 180 feet and a diameter of 110 feet seem adequate for the concept.

In the size of 1000 mwe or larger there is reasonably good indication that such a unit may be competitive with conventional plants burning coal at 25 cents per million Btu. A preliminary estimate of the power cost of a 1000-mwe SCOTT-R, for example, is shown in comparison to a conventional plant in Table II. The SCOTT-R fuel cost is based on the AEC uranium price schedule and 4¾ percent inventory charge, which have been the effective ground rules since July, 1962, and anticipated fabrication costs.

Development Areas

The attractive economic potential of a supercritical once-through tube reactor (SCOTT-R) cannot be achieved unless the technological understanding of high-temperature, high-pressure reactors and materials is extended through extensive development effort. The first step in such a development program is to identify the problems. Undoubtedly, as work proceeds, new problem areas will arise, but the following areas are anticipated to be critical to the overall success of the program:

1. A dependable pressure tube, comprised of low-neutron cross-section material for service at relatively high-temperature and high-pressure operation, must be developed.
2. Long-life fuel elements having advanced thermal design criteria must be developed and proven.
3. The problem of corrosion and contamination must be resolved in order to employ the direct cycle system. Corrosion rates under long-time operating conditions must be acceptably low to avoid fuel-cladding failure and turbine contamination problems.

Pressure-Tube Considerations—The pressure tube is an integral part of the core. Consequently, the usual high-strength materials cannot be effectively used because of their characteristically high neutron absorption cross sections. The design of the pressure tube is critical to the feasibility of the concept. Not only is the capital cost affected, but, inasmuch as the pressure-tube walls are integral with the reactor core, the fuel cost can be adversely

Table III THE FOUR PHASES OF DEVELOPMENT

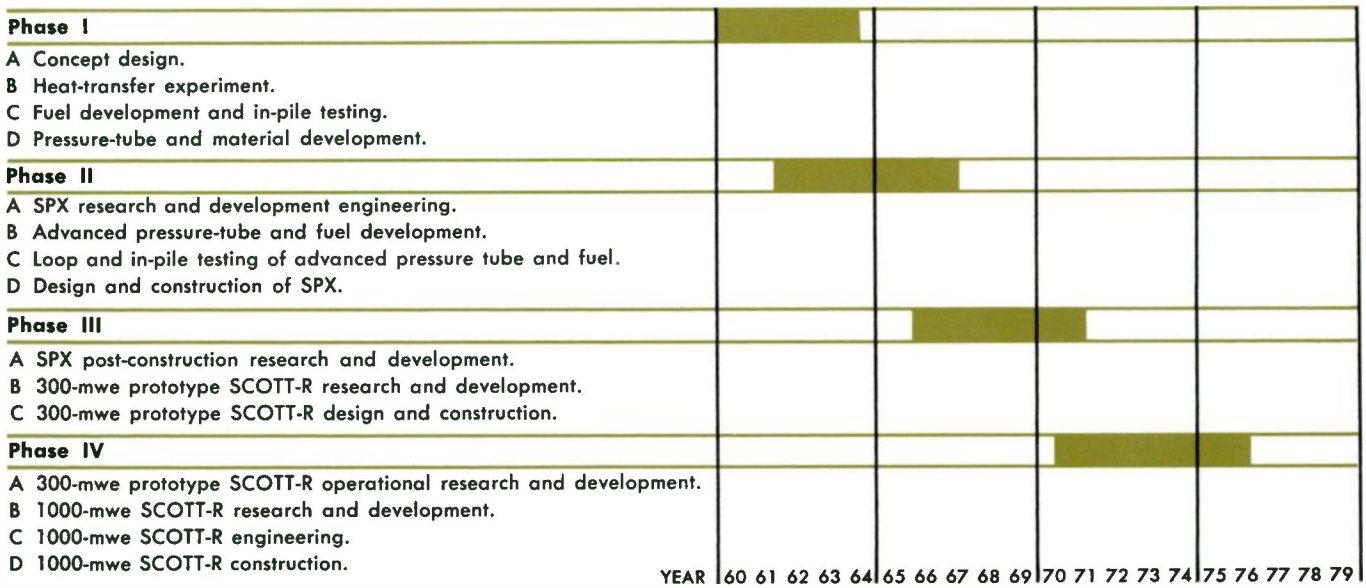

affected by improper selection of the material and design.

If the SCOTT-R concept is to have an economic advantage, a low-neutron cross-section material must be used in the high-pressure section of the core. Zircaloy is a preferred material for the pressure tube in this section. With a reentrant tube design (Fig. 4), the temperature of the tube can be maintained low enough so that its strength and corrosion characteristics are acceptable.

Fuel-Element Development—The nuclear superheat fuel assembly is a critical item with many uncertainties and potential problems. The fuel element must operate with high surface temperatures if it is to achieve good thermodynamic performance. Typically, the surface temperature of a fuel element varies over its length as a function of the core power distribution and the heat transfer properties of the steam coolant, so that the peak surface temperatures of 1200 to 1300 degrees F are often necessary to achieve 1000 to 1100 degrees F outlet superheated steam temperatures.

These high temperatures require a new concept in fuel cladding. The rather thick free-standing cladding, commonly employed in dry- and saturated-reactor systems, is not practical when the cladding material is operating at temperature levels in the creep range. Operating temperatures and economics dictate that "collapsed" cladding must be used, with the ceramic fuel itself serving as the support that resists the external coolant pressures. This raises numerous problems of feasibility and performance that must be answered.

The technology of designing and fabricating sound fuel elements of both rod and annular shapes will require much development. On the whole, the problems of rod-type fuel, assembled in clusters of rod bundles, appear less formidable because of the large base of existing technology. However, annular fuel elements assembled in concentric ring pattern appear to have important performance advantages, chiefly in reduced volume of cladding material and better heat-transfer characteristics.

Corrosion and Contamination Problems—Another serious feasibility problem is the selection and performance of the reactor materials. In a once-through, direct-cycle reactor there is no means whereby radioactive corrosion products, water impurities, and fission products can be removed once they have entered the coolant stream. Contamination of the turbine, condenser and feedwater heaters is a problem of serious proportions. Materials and operating procedures must be selected to effect a satisfactory solution to the problem. Fuel elements, pressure tubes and feedwater heaters are items of primary concern.

The problem of corrosion and mass transfer of radioactive materials may be quite severe in a large direct-cycle once-through plant. For example, with temperatures and heat fluxes expected of the superheat fuel elements, a target objective is to obtain fuel cladding having a corrosion rate of 10 mg/dm^2/mo or less. Even though this is a small number it accounts for a large amount of corrosion-product production over a year's time. For a typical average heat flux, a 1000-mwe reactor might be expected to produce in the range of 80 to 100 pounds per year of corrosion product. If this product is retained on the fuel surface, no contamination problem will occur; reduction in the heat-transfer coefficient is the only result. On the other hand, if corrosion products become highly radioactive and then break away from the fuel-cladding surface to be carried away in the stream, a problem of rather sizeable proportions may develop in the condenser hotwell or in the purification systems. Furthermore, if the fuel-cladding integrity is insufficient to retain the fission products, additional contamination could result from their release and distribution. Chloride stress corrosion is a key problem receiving much attention at present. Development effort directed toward the solution of these important problems will determine the eventual feasibility of direct-cycle superheat systems.

Development Program

The successful demonstration of an economically attractive supercritical-pressure, once-through tube reactor con-

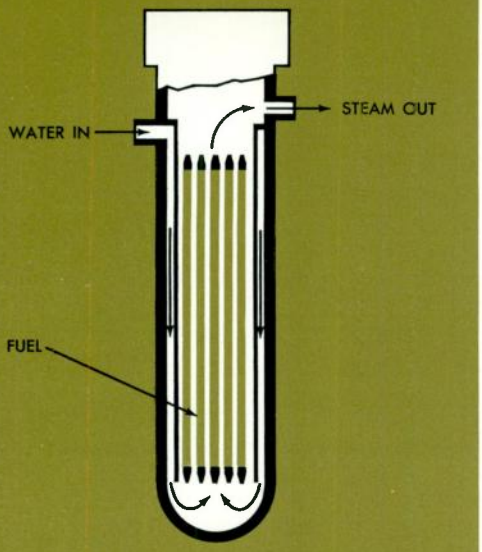

Fig. 4 In reentrant-type pressure-tube design, coolant flows through a baffled annular space between the tube wall and the fuel and then up through the fuel region.

Table IV PLANT DATA SHEET FOR THE SPX

Power Rating	Reference Core Rod Elements	Alternate Core Annular Elements
Total Thermal Power, mwt	39.81	54.34
Thermal Power Steam, mwt	38.57	52.65
Moderator Power, mwt	1.24	1.69
Coolant Conditions		
Outlet Steam Temperature, °F	1000	1000
Outlet Steam Pressure, psia	3500	3500
Feedwater Temperature, °F	500	500
Feedwater Pressure, psia	3565	3750
Total Steam Flow, 10^6 lbs/hr	0.141	0.1918
Reactor Core		
Core Diameter, ft	6.24	6.24
Active Core Height, in.	141.8	141.8
Length/Diameter Ratio	1.90	1.90
Fuel Weight, UO_2, lbs	7350	9310
Initial Enrichment, a/o	6.02	5.5
Burnup, MWD/Tonne	10,000	10,000
Lifetime Rated Power, FPH	17,850	16,500

cept requires an extensive development effort. The Westinghouse Superheat Development Program has been established for this purpose. It is a long-range integrated program that culminates in the design of a large (1000-mwe) reactor. During the course of the program, the construction and operation of both a Superheat Power Experiment (SPX) and a 300-mwe prototype (SCOTT-R) are envisioned. The major steps in the program are: (a) Conceptual design studies, (b) out-of-pile test and development, (c) in-pile test and demonstration, (d) design, construction and operation of SPX, (e) design and construction of a power prototype, (f) design of SCOTT-R in large size. These steps are grouped into four phases as shown in Table III, which includes the approximate schedule of development.

The objective of the Phase I program is an evaluation of the feasibility problems and ultimate potential of the SCOTT-R concept. Development work in supercritical heat transfer experiments, design, fabrication and in-pile testing of fuel and pressure tubes and materials development are included in this basic program.

The second phase is directed to the development and construction of an experimental facility to test fuel components and systems concepts. The preliminary design of this facility is completed. It is designed to develop 50 thermal megawatts to produce steam at 3500 psi and 1000 degrees F. The facility will be flexible in operation to explore higher steam temperatures, in-core reheat application, and once-through subcritical performance.

SPX has a nominal rating of 50 mwt and produces supercritical steam at 3500 psia and 1000 degrees F. The power-producing unit of the experiment is a graphite-moderated nuclear reactor in which the fuel is contained by reentrant pressure tubes and cooled by circulating supercritical water. The plant is not intended to produce electric power but will reject heat to a heat sink—a cooling tower in this design, since natural cooling water was not available for the site considered. Fluid systems and component designs are planned to permit substantial deviation from nameplate operating conditions to provide maximum possible information return per unit of capital investment. The design of systems and components are retained within current technology to reduce time delays and capital outlay.

Fuel to produce the 50 mwt nameplate power rating for the SPX is contained in 44 reentrant pressure tubes, which penetrate the top head of a cylindrical stainless steel reactor vessel. Space for eight additional pressure tubes is provided around the periphery of the core to allow incorporation of an integral nuclear steam reheat experiment. The reactor vessel is internally insulated and externally cooled by contact with the water surrounding it in the neutron and thermal shield tanks. The principal plant and core parameters are shown in Table IV.

The third phase of the program will incorporate the analysis of operational data from Superheat Power Experiment in parallel with the development, design and construction of prototype reactor.

This reactor will be designed to produce power on a reasonably economic basis while prototyping all the aspects of large plant operations. The size selected to resolve both of these requirements is 300 mwe. The schedule calls for operation in the early 1970's.

From the information gained in the development and operation of the power experiment and prototype reactor, the design and construction of the large plant can proceed with high technical surety. Some additional development will be required to resolve the problems of increased size as well as improved performance in fuel, pressure tubes, and general cost reduction.

This program is time consuming and costly; there are numerous feasibility problems that could impair its economic potential and even its performance characteristics. The objective, however, of a highly efficient nuclear steam plant producing power competitive with average fossil fuel costs in the U.S. is sufficiently attractive to justify the development effort required.

The Case for EHV Transmission

The move to 500-kv transmission has come because of recent economic justification—the technology has existed for some time.

J. K. Dillard Manager, Electric Utility Engineering Department, Westinghouse Electric Corporation, East Pittsburgh, Pennsylvania
E. W. DuBois Sponsor Engineer, Electric Utility Engineering Department, Westinghouse Electric Corporation, East Pittsburgh, Pennsylvania

The decision to build the nation's first commercial 500-kv transmission system was disclosed in early 1962. Several additional 500-kv projects have been announced since. With these developments underway, two questions arise: Why are the utilities now moving to 500 kv? And if the idea is sound, why has the industry waited so long?

Critics of the American power industry claim that the United States lags Russia in the development of extra-high-voltage (EHV) transmission. They point to the 500-kv ac lines already operating in Russia, and to the ±400-kv dc Volgograd-Donbass line projected for operation in the future. Certainly, these projects demonstrate achievement in securing high operating voltage levels. However, there are more important measures of progress in power transmission, such as reliability, availability, and cost of energy to the ultimate consumer. When these factors are considered, the American power industry comes out well ahead.

Minimum Revenue Requirements

Recent reports in the technical press[1] indicate that the Russians are beginning to recognize the economic fallacies that led to the development of remote hydro projects and long-distance EHV lines too soon. A Russian economist has stated that the fallacy is their omission of capital costs in evaluating alternative projects. The error has resulted in miscalculation of the over-all costs to the economy and has favored projects with excessively high capital costs. Because of our free market conditions and our recognition that capital costs something, the American power industry has not fallen into this same pitfall in the development of EHV transmission systems. Rather, transmission expansion in the United States has been careful and measured, keeping step with needs for higher voltages as determined by costs of reliable service to the ultimate consumer. Many U.S. utilities use the economists' concept of "minimum revenue requirements" to pick the most economical alternative for system expansion. Therefore, instead of being a goal in itself, each move to a new EHV (over 230 kv) level has resulted from economic need.

Transmission voltages in this country have progressed from 10 kv in 1892 to 345 kv in 1962, as shown in Fig. 1. The first EHV line was put into operation at 287 kv in 1935 from Hoover Dam to Los Angeles. Eighteen years later, in 1953, the first 345-kv lines were put into service. Today over 3000 miles of 345-kv lines testify to the need for EHV

Fig. 1 History of high-voltage transmission.

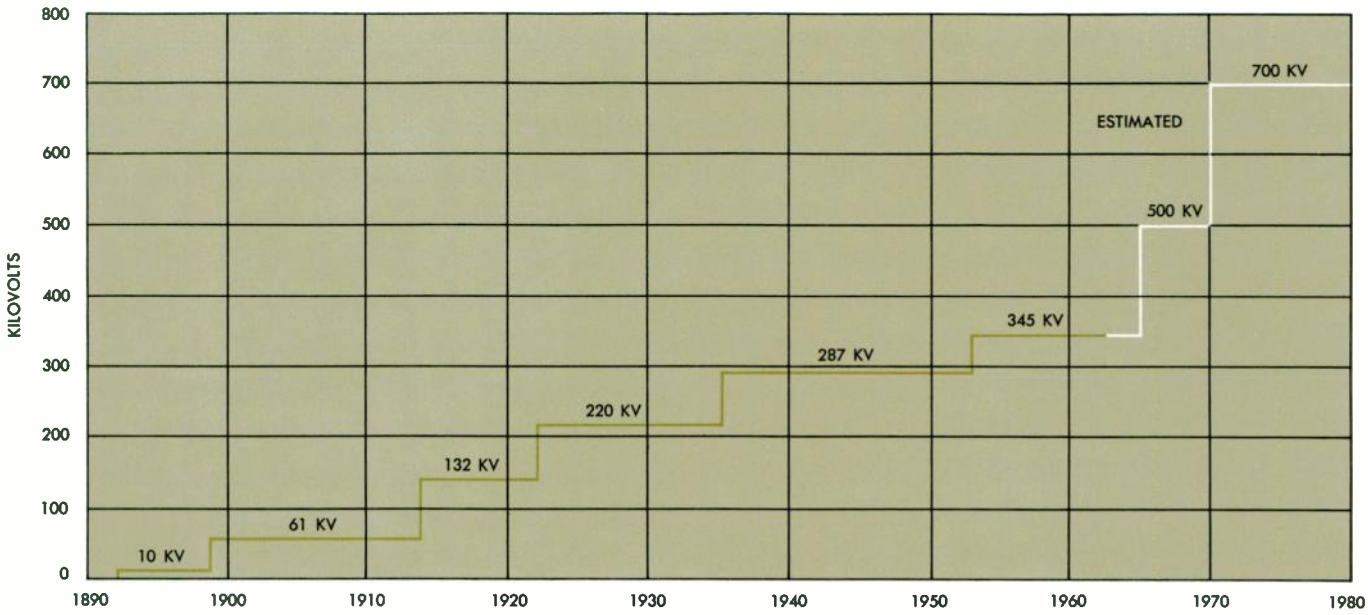

transmission. Now the next step in transmission voltage to 500 kv is in progress, again based on sound economic justification. The United States is at the threshold of a major move to 500 kv in many parts of the country.

The Virginia Electric and Power Company and Westinghouse are presently engineering the nation's first 500-kv commercial circuit. Two sections amounting to 180 miles of line will be energized in late 1964. The following year the terminals will be connected in a loop, making a total of 350 miles of line in operation. With other 500-kv projects that have been announced, or will be announced in the near future, about 2000 circuit miles of 500-kv transmission will be in service by 1967.

500-kv Technology

Technology for moving to 500 kv has existed for many years. Field testing programs at 500 kv have been carried on continuously since 1946. The first major EHV experiments in this country were conducted at the Tidd Project. This test line was operated from 1946 to 1953 to study corona, radio influence effects, and insulation problems on EHV lines and terminal equipment. The Tidd tests provided the basic engineering data for the 345-kv transmission circuits, and demonstrated that 500-kv transmission posed no basic problems that could not be solved.

The next major field test facility was the Leadville High-Altitude Project. In tests conducted from 1956 to 1961, the effect of altitude on radio influence, corona, and other major factors influencing line design was evaluated. As a result of these tests, smaller conductors will be applied to EHV lines at all altitudes above sea level.

Today, the Apple Grove Project is extending the investigations to transmission voltages in the range from 500 kv to 775 kv. These research investigations have provided the basic engineering data required for any voltage requirements of the next 20 years.

Technically, the use of higher voltages permits the transfer of larger blocks of power because transfer capability increases approximately as the square of transmission voltage. Transmission engineers use the concept of surge impedance loading (SIL) to define the permissible power transfer capability of any circuit for various transmission distances.* The curves of Fig. 2, developed from studies based on this concept, show the dramatic increase in power transfer capability at higher voltages.

Since the technology has existed for some time, why has the American power industry waited until now to move to 500 kv? Simply because the economic reasons for moving to a higher voltage level did not previously exist. These reasons have to do with the load growth that has occurred since the move to 345 kv, and the size of the blocks of power that now need to be shifted between power systems.

Voltage Level vs. Economics

Changes in voltage level are rarely, if ever, justified by short-term growth predictions. When studies are limited to two or three years, the results invariably show that lowest revenue requirements are obtained by staying at

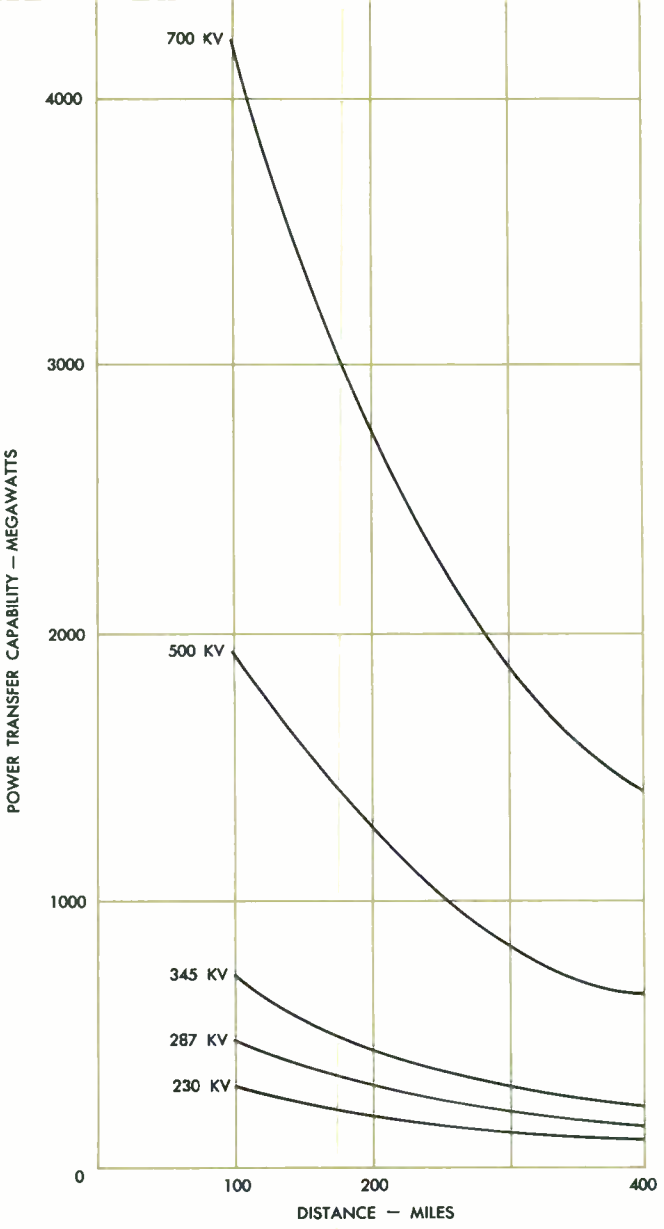

Fig. 2 Permissible line loading, as determined from the surge impedance loading concept.

existing voltage levels. However, if studies are projected far enough into the future—say ten or twenty years—a higher voltage level is often justified on a present-worth basis. Only recently have new planning techniques been developed sufficiently to permit utilities to look substantially ahead in an intelligent way.[2,3] These techniques now permit utilities to justify higher voltage levels on economic grounds with confidence.

If a transmission system is to be developed most economically, voltage steps must be neither too big nor too small. In general, a system with 230-kv transmission will find it most economical to stay at 230 kv until growth and pooling requirements dictate 500 kv as an economical level. Similarly, 345-kv systems will probably bypass 500 kv in favor of 700 kv when growth and power transfer requirements between systems dictate a higher voltage level.

The present moves to 500 kv reflect the economic needs of power systems with top voltage levels now of 230 kv.

*SIL = 2.5kv² for single conductor lines, or 3.0kv² to 3.9kv² for bundled conductor lines. Capability for a 100-mile line is 2.0 SIL, a 200-mile line is 1.5 SIL, and a 300-mile line is 1.0 SIL. Lines less than 100 miles long may be loaded as high as 4.0 SIL.

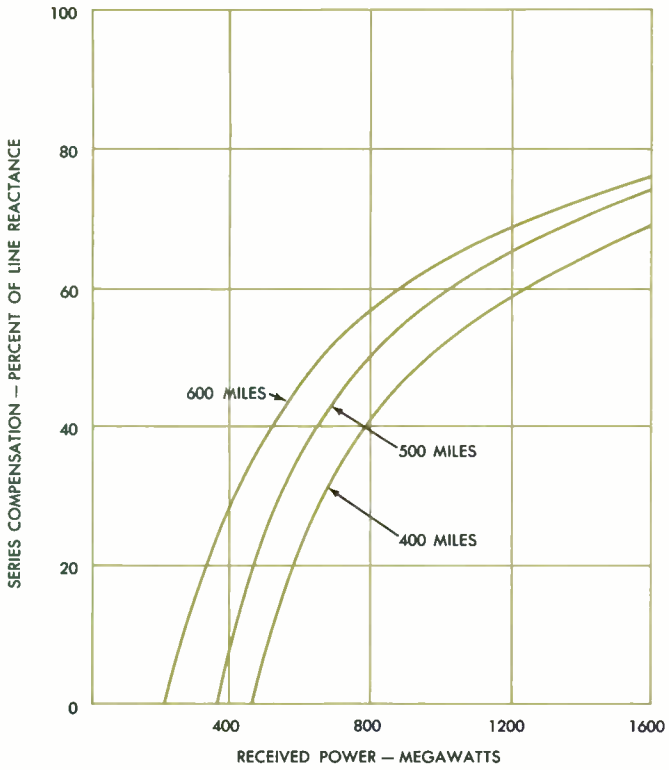

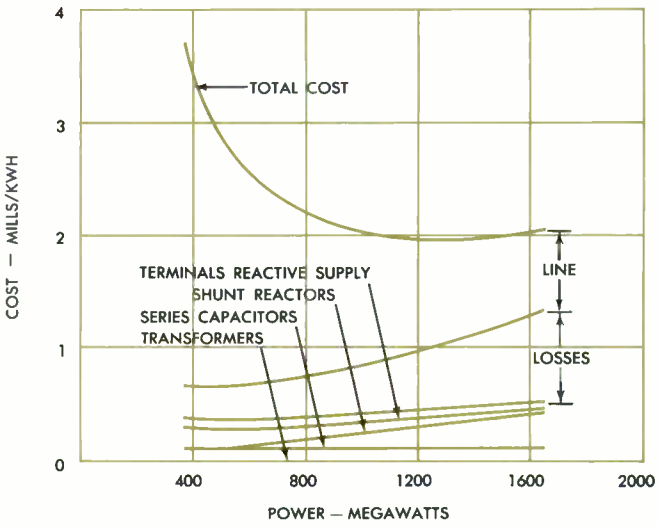

Fig. 3 (Left) Series compensation requirements for 500-kv transmission.

Fig. 4 (Above) Component transmission costs for a 500-mile, 500-kv line, operated at 70 percent load factor.

Fig. 5 (Right) Transmission cost for optimum circuit loading of (a) 500-kv and (b) 700-kv lines. (The economic assumptions used to develop these costs are shown in Table I.)

The exact reasons for the attractiveness of 500 kv vary for each system. In some cases, the prevailing factor is the optimum use of existing or limited rights of way. However, this is usually only a factor in metropolitan areas having short lines loaded to three times their SIL, or more. In other cases, the decisive economic factor is the utilization of remotely located, low-cost energy sources (e.g., mine-mouth generation or hydro). For these projects, EHV is used for straightaway transmission, and simple calculations of mills/kwh are adequate for comparison with alternate methods of energy transportation.

But EHV transmission is justified most often for interconnections between two or more separate power systems to achieve sharing of installed reserves, construction of larger plants, interchange of economy energy, and development of integrated EHV systems and grids. Comparisons of simple mills/kwh for various transmission circuits are not adequate in these situations. Over-all system planning studies, using the new techniques mentioned above, are needed to determine the block sizes of power transfers, the integrated economic dispatching of energy, and the transmission grid necessary to accomplish these interchanges of kilowatts and kilowatt-hours.

Extra-Long-Distance Transmission

Operational flexibility and low transmission costs are strong incentives for serving expanding loads from close-in generating stations. However, increases in the cost of delivered fuel can make alternative plans attractive in some areas of the country where fuel prices are already high.

When considering the use of remotely-located low-cost energy sources, a number of alternative energy transport methods must be thoroughly evaluated. Extra-long-distance (ELD) transmission must compete with coal transport by rail, barge, or pipeline, or with atomic power plants that can be located much closer to the load. (ELD transmission refers to distances in excess of 400 miles.) Fuel quality, basic fuel cost, and the character of the existing system influence the ultimate choice of alternatives.

The basic energy transfer requirements for remote energy projects are well defined in terms of distance, ultimate power level and sequential development of the facilities. These considerations uniquely determine an optimum voltage level for electrical transmission. Since the distances involved are long by definition, large amounts of power transfer at relatively high load factors are required for economic feasibility. High power levels and long distance inherently imply EHV transmission, again on economic grounds. Complete freedom is not available in the choice of voltage because it is desirable to work within the framework of standard voltage levels.

The technical feasibility of ELD lines depends upon the use of shunt reactors to control dynamic voltages along the line and upon series capacitors to increase power transfer. The amounts of shunt and series compensation required for ELD lines extend far beyond the conventional experience of the system planner.[4] To achieve economic loading of facilities, series compensation up to 80 percent of line reactance is required. For example, the series compensation requirements for 500-kv transmission over distances of 400, 500, and 600 miles is shown in Fig. 3.

In ELD transmission, optimum economic loading at a given operating voltage is relatively independent of transmission distance. The optimum power level in terms of mills per kwh transmission cost at 500 kv can be determined from a series of curves similar to the total cost curve of

a

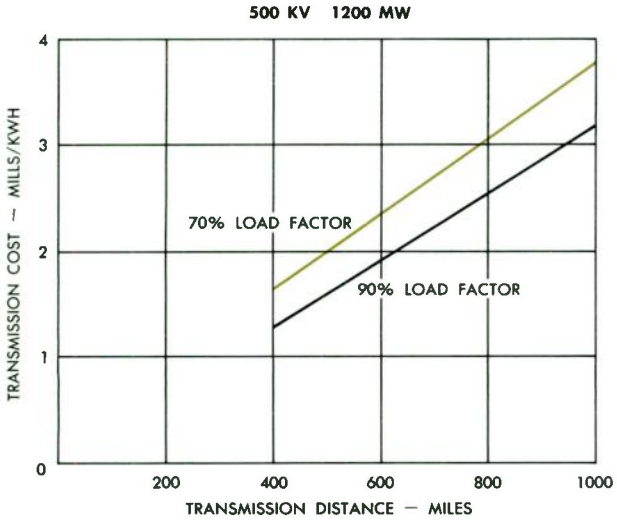

b

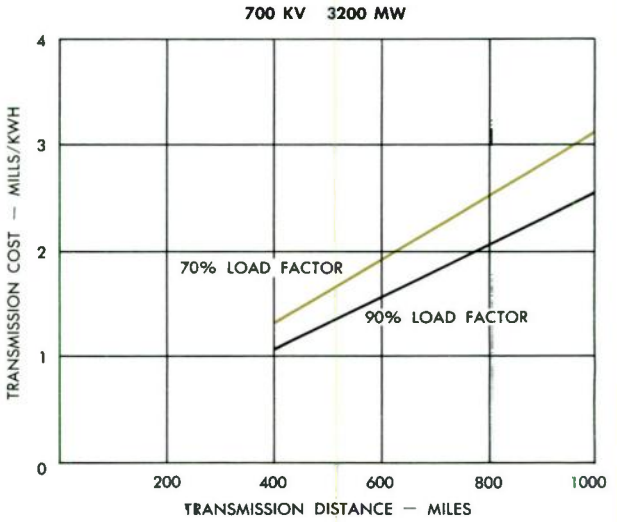

Table I ECONOMIC ASSUMPTIONS

	500 KV	700 KV
Line Cost Including R-O-W	$90,000/mile	$175,000/mile
Autotransformers (230-kv/500-kv) (345-kv/700-kv)	$2/kva —	— $3/kva
Breaker Position (2 breakers per line section)	$500,000 each	$1,000,000 each
Shunt Reactors	$4/kva	$7/kva
Series Capacitors	$7/kva	$7/kva
Receiving End Reactive Supply	$7/kva	$7/kva
Losses-Demand and Energy Charge	$25 plus 2 mills/kwh	
Annual Transmission Investment Cost	15% (including operation and maintenance)	
Load Factors	70% and 90%	
Loss Factors	58% and 85.5%	

Fig. 4. The minimum cost point corresponds to a power level of approximately 1200 mw. Similar curves drawn for other distances in the ELD range and utilizing the same assumptions have minimum cost points at roughly the same power level. In contrast, comparable treatment of 700-kv transmission indicates an optimum economic power level of 3200 mw per circuit.

At a given voltage, the unit cost of transmission associated with the optimum economic power level varies almost linearly with distance. The behavior of the unit cost function for 500-kv and 700-kv transmission is presented in Figs. 5a and 5b. Seventy and ninety percent load-factor curves are plotted to show the effect of reduced usage. The economic assumptions used to develop Figs. 4 and 5 are given in Table I.

The concept of optimum economic loading is important. The cost of transmitting 1200 mw a distance of 500 miles at 70 percent load factor is approximately 2 mills/kwh for 500 kv. The unit cost of transmission for these conditions using 700 kv would be 2.6 mills/kwh, an increase of 30 percent. However, if the 700-kv line is operated at 3200 mw, its optimum loading, the unit cost is 1.65 mills/kwh. In the latter case, the receiving system must absorb up to 40 billion kilowatt hours per year. By comparison, the total energy sales recorded by the United States electric industry in 1960 was slightly in excess of 684 billion kilowatt-hours.

Other interesting facts can be drawn from Fig. 4. The total cost curve is relatively flat in the minimum cost area. This is characteristic of this type of curve in the ELD range. Thus, power levels can deviate from optimum without severely affecting the choice between alternatives.

A breakdown of the major cost components associated with ELD transmission as a function of transmitted power

REFERENCES
[1] "Soviets Find Capital Costs Make Hydro Less Economical," *Electrical World*, August 20, 1962, pp. 56–59.
[2] "The Utilities Trend: Growth and Pooling," J. K. Dillard, *Mechanical Engineering*, vol. 84, no. 11, November 1962, pp. 60–64.
[3] "System Simulation," J. K. Dillard and C. J. Baldwin, *Westinghouse ENGINEER*, September 1960, p. 130.
[4] "Extra-Long-Distance Transmission," E. W. DuBois, J. F. Fairman, Jr., D. E. Martin, C. M. Murphy, J. B. Ward. *AIEE* Paper 61–793.

for the 500-mile case is given in Fig. 4. Taking the component costs at the optimum loading point of 1200 mw, the breakdown of the total transmission cost of 1.98 mills/kwh is:

Component	Mills/kwh	Percent of Total
Line	0.980	49.5
Losses	0.575	29.0
Shunt Reactors	0.055	2.8
Series Capacitors	0.214	10.8
Reactive Supply	0.050	2.5
Transformers	0.106	5.4
Total	1.980	100.0

For this evaluation, the line cost was taken at $90 000 per mile, including right-of-way. Nearly half of the total cost of 500-mile, 500-kv transmission is represented by line plus right-of-way cost.

ELD transmission is justified in few locations in the U.S. Almost all low-cost coal sources in the East are less than 400 miles from the large load centers. Furthermore, the transmission complex dictates consideration of interconnections in combination with resource utilization.

In the West, coal reserves in Utah, Wyoming, and New Mexico are plentiful and far removed from load centers. For such projects, the transmission costs of Figs. 5a and 5b can be converted to fuel cost differential curves. For generating units with over-all heat rates of 8500 Btu/kwh, the fuel cost differentials to justify various 500-kv transmission distances at 90 percent load factor are:

Miles	Fuel Cost Differential in Cents Per 10^6 BTU
400	15.2
500	18.7
600	22.2
700	25.7

Some major remote hydro sources still exist in the West also. In the fundamental evaluation of these resources an economic threshold exists beyond which the use of the resource is not justified within the framework of present technology and alternative costs. It is questionable that hydro can compete with 6 mills/kwh nuclear plants located at the load center if the hydro resource is located 700 miles away. To arrive at this limiting distance, the cost of generation was assumed to be $25/kw/yr. The basic transmission costs were taken from the 70 percent load factor curves of Fig. 5, except that no charge was made for the energy component of losses.

System Interconnections

Electric utility companies have taken advantage of high-capacity system interconnections for many years. Early ties were made as insurance against catastrophe. Gradually, neighboring utilities began to use these interconnections for economy interchange during off-peak periods. Such operation has resulted in significant savings in production expense. In recent years, there has been great activity in the alignment of power pools for mutual planning for new facilities. These plans are aimed toward taking increased advantage of economy interchange, lower installed reserve requirements, delay of unit installation, and the lower dollars/kw cost associated with larger units.

The choice of transmission voltage for high-capacity interconnections is not as simple as that for point-to-point transmission. Judgment is an important factor with respect to growth rate of the systems, anticipated individual system development, and future interconnection possibilities. The selection of the appropriate voltage level for an EHV tie cannot be made until the full benefits of integrated operation are evaluated over a long-term period.

The cost of EHV transmission between systems can be a major economic factor in system expansion plans. Therefore, the use of the EHV tie to carry emergency reserve and economy interchange must be evaluated, and the costs of providing the required tie capacity at different voltage levels must be determined. Only when the annual revenue requirements for transmission investment are combined with revenue requirements for generating plant and production expense can total revenue requirements for the pooling arrangement be minimized. Therefore, the decision of voltage level for an EHV interconnection between two systems really cannot be made until line use is analyzed with regard to both emergency power transfer and economy energy transfer in future years. Such an analysis requires consideration of installed generation plans on the system and its neighbors, the value of ties to both neighbors in delaying generation installations, and economies possible through common economic dispatch of the two systems. Hence, the choice of tie line voltage level must go beyond a dollars-per-kilowatt or mills-per-kilowatt-hour type of evaluation.

New digital computer planning programs (such as the Westinghouse Powercasting technique) simplify the planning for power pools and EHV lines. The new methods and programs use the technique of simulation to evaluate installed reserve savings, operating savings from economy interchange, transmission ties needed between systems, optimum voltage levels, new optimum unit sizes for the pool, and new optimized long-range expansion patterns.

Powercasting studies conducted to evaluate the economies of a number of pooling arrangements have shown savings that vary from three to ten percent, or more, of the present worth cost of the expansion pattern. The savings expressed in dollars are even more impressive. The results for a study of one pool, to be made up of several separate companies with a present generation capacity of about two million kilowatts, showed savings in excess of $9 000 000 per year on a levelized basis. Dollar savings amounted to approximately ten percent of the present worth cost of the expansion pattern.

The Case for EHV

Pools and systems differ and specific studies are required for each pooling arrangement to ascertain the true level of benefits accruing to pool operation. Comprehensive studies are fully worth the relatively small cost of conducting them because of substantial savings that can be realized. The point to be made is that the real incentives for EHV transmission lie in the area of high capacity interconnections. The technology exists today to build transmission systems up to the 700-kv level. Recognizing these facts, utilities will build extensive EHV transmission facilities in the next few years to implement regional interconnection plans.

Filters in Electronics

Anatol I. Zverev
Network Synthesis
Electronics Division
Westinghouse Electric Corporation
Baltimore, Maryland

Many of our most sophisticated accomplishments in electronic equipment design are a direct result of developments in electric wave filter technology.

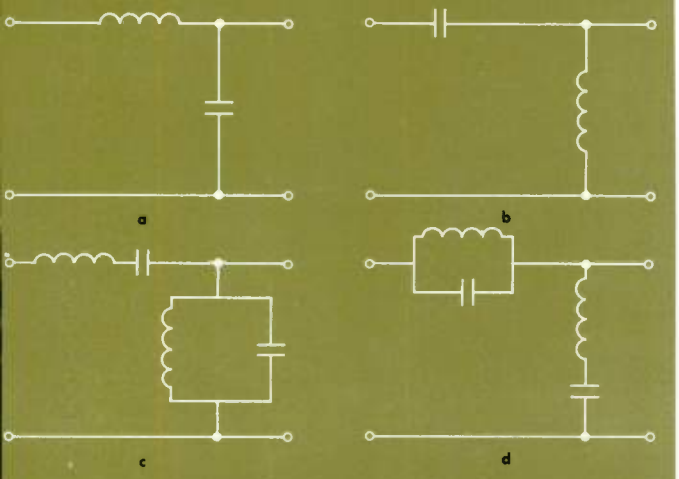

Fig. 1 Examples of the four fundamental electric wave filter types: (a) Low-pass filter; (b) high-pass filter; (c) band-pass filter; and (d) stop-band filter.

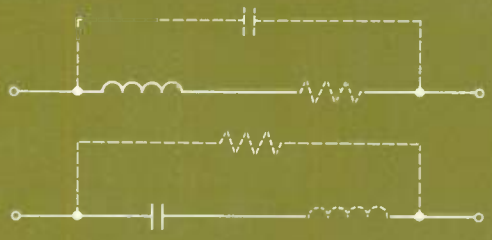

Fig. 2 The equivalent circuit of an inductor and capacitor, when losses and parasitic reactances are considered.

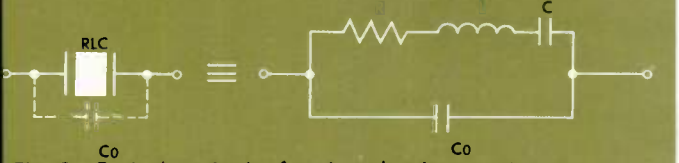

Fig. 3 Equivalent circuit of a piezoelectric resonator.

Today's progress in electronics is closely related to advances in filter technology and network theory. Electric wave filters are used to channel energy, divide the frequency spectrum, extract frequency-shift information, integrate coherent signals, and maintain the accuracy of separation between frequency sources. Performance of passive and active networks, in the form of transmission filters, can be predicted and analytically described under actual operating conditions in an exact mathematical form. This fact explains the emphasis that has been placed on the filters which are frequency selective networks in new electronic systems. Electronic circuit designers prefer to synthesize passive networks for the entire system whenever possible.

Types of Filters

Four basic types of frequency-selective networks are used in electronic equipment:

1) The *low-pass filter* transmits electric wave energy from zero frequency up to a certain cutoff frequency, and attenuates or rejects wave energy at frequencies beyond this limit. (Loosely, a low-pass filter can be said to transmit low frequencies and reject high frequencies.)

2) The *high-pass filter* rejects frequencies below cutoff, and transmits frequencies above this frequency.

3) The *band-pass filter* transmits a band of frequencies between a certain lower and upper limit, and rejects frequencies outside this band.

4) The *band-reject filter* rejects a band of frequencies, and passes all others.

Electrical filters can be classified in many different ways. Depending on the circuit configuration of the basic elements, they are called *ladder* filters (in the form of π-filters or T-filters) or *lattice* filters. Depending upon the character of the elements, filters are classified as: LC filters, where the basic elements are capacitors and inductors; RC filters, where the elements are capacitors and resistors; transmission-line filters and stripline filters; coaxial filters, piezoelectric filters, electromechanical filters, magnetostrictive filters, etc. If a filter has a source of energy within the network, the filter is an *active* filter; those with no source of energy within the network are termed *passive*.

The Elements of the Filter

The fundamental elements of filters are the reactances—lumped capacitance and lumped inductance. Some types of filters can be designed using only capacitors and resistors—this combination is especially useful in active filters—but the normal passive filter requires both inductance and capacitance. The simplest filter consists of a series arm and a shunt arm (Fig. 1). It is a low-pass filter if the series arm is an inductor and the shunt arm is a capacitor; it is a high-pass filter if these reactances are reversed. The simplest forms of band-pass and band-reject filters are shown in Fig. 1c and d.

To a first approximation, lumped inductance and capacitance can be considered as a pure reactance; actually, two more quantities are present—losses and parasitic reactance (Fig. 2). Although losses are low in comparison with reactance, they cannot be neglected, especially in the design of narrow-band filters or sharp response curves. Losses tend to give a drooping response and increase the attenuation within the pass band. Parasitic reactance in lumped com-

ponents causes distortion of the network response and may even destroy the response altogether if not neutralized or properly taken into consideration.

The conventional measure of quality of a reactance is the quality factor, Q. This factor is simply the ratio of the reactance (of a coil or capacitor) to series resistance. Common values of Q in the conventional inductors at radio frequencies are 50–300; similar value for capacitors at these same frequencies are usually 500–5000. The higher the Q factor, the better the filter that can be designed.

The demand for high Q factors in ordinary lumped components, especially coils, has intensified the search for substitutes for the inductor and capacitor. The first and the most successful substitute was the piezoelectric crystal.

The equivalent schematic of a piezoelectric resonator is shown in Fig. 3. There are three reactances in the first approximation: L and C are the motional parameters, and C_o is a capacitance across the crystal and can be considered a parasitic parameter. The piezoelectric resonator has a Q factor of several thousand, and is very stable with time and environmental conditions. With such resonators, filters of high selectivity and with vanishingly small bandwidths can be developed.

However, the piezoelectric crystal exhibits, in addition to the primary mode, other modes of oscillation which are unpredictable and undesirable. The latter modes are a serious limitation of ordinary crystals, as some of these spurious modes are close to the fundamental frequency. Another limitation of crystals for filter application is the fact that the ratio between the parasitic capacitance (C_o) and motional capacitance (C) cannot be made less than a certain value. The value of this ratio limits the bandwidth that can be obtained. In the low frequency range (up to 200 kilocycles) this bandwidth can be no more than about 10 percent; at higher frequencies, the percentage bandwidth is less, and at 30 megacycles it can be only a fraction of one percent, even when all supplementary measures are taken into consideration.

Therefore, because the crystal is a very narrow band device, has spurious oscillation, and the physical size is so small at high frequencies that the fundamental mode is impossible to obtain, crystal resonators function best in the frequency range of several kilocycles up to 20 mc.

The value of lumped inductance and capacitance to produce resonant circuits in the VHF range (30 to 300 megacycles) is very small, and associated parasitic components will radiate energy and reduce the Q factor. Therefore, distributed resonators become increasingly important components at VHF frequencies and above. For example, the simplest form of distributed resonator is a length of symmetrical (or coaxial) line. This resonator can be used not only as a transmission system, but also as a filter element. A single transmission line possesses distributed inductance, capacitance, and distributed losses. The resonant frequency is determined by not only these values but by line length, as illustrated in Fig. 4. The impedance of the transmission line can behave as a capacitance, an inductance, a series resonator, or a parallel resonator depending upon the relationship between the length of the line and the wavelength. Two-terminal networks made from sections of coaxial line have relatively high Q factors (1000 and up) and are especially useful for UHF frequencies (300 mc to 3 kmc).

One of the most practical filters for VHF and UHF frequencies is the coaxial resonator. The conventional coaxial resonator is a cavity with a center post (Fig. 5a). Energy is introduced into the cavity by means of inductive loops, capacitive probes, etc. Output is provided with similar coupling arrangements. Conventional coaxial resonators are generally used for filters within the range of 200 mc to 5–6 kmc. This covers part of the VHF range, the UHF range, and the microwave range.

The Q factor of the coaxial resonator is usually very high and sufficient for most high-quality filters. However, in the VHF range, coaxial construction becomes bulky and unproportionally large in comparison with electronic tubes, transistors, and other components of modern circuitry. For example, the length of a quarter-wave resonator, at 100 mc, is about 30 inches.

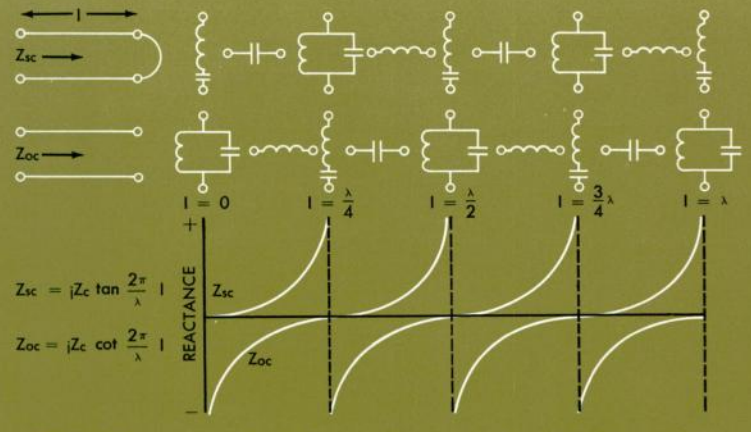

Fig. 4 Two symmetrical lines are shown, one terminated in a short circuit, the other in an open circuit. The input impedance of such lines, with negligible losses, is a function of length, and can be expressed as a trigonometric function; the first as tangent and the second as cotangent of the same argument.

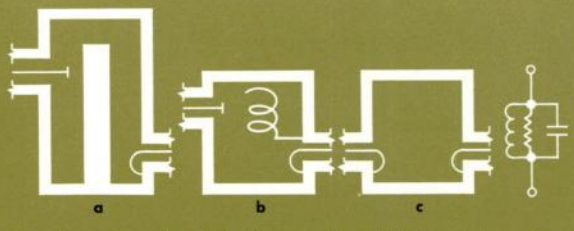

Fig. 5 Filters for high frequencies: (a) Coaxial cavity with capacitive probe and inductive loop coupling; (b) helical resonator; and (c) waveguide cavity, with a single mode equivalent lumped-parameter circuit indicated.

Fig. 6 (Below) Stripline filter arrangements. Shown is the center conductor which is sandwiched between a dielectric material. This combination is then sandwiched between two conducting ground planes.

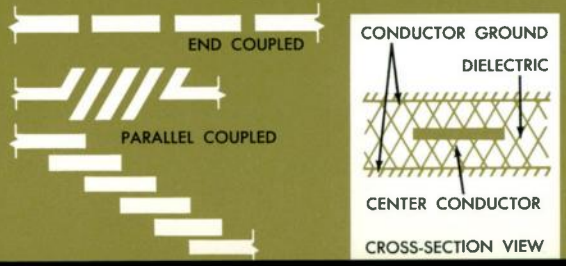

The helical resonator, shown in Fig. 5b, is similar to the quarter-wave coaxial resonator except that the inner conductor is in the form of a single layer solenoid. Its Q factor in the VHF range is from several hundred to 1000. The helical resonator occupies what once was "no man's land" —the 20–500 mc region where lumped elements and crystal resonators become ineffective, and coaxial cavity resonators are too large to be practical. The helical resonator can be useful even for higher frequencies when a Q factor between several hundred and 1000 is sufficient. Helical resonators are best built in a square block design for the highest quality filter. These filters can be used equally well for narrow-band or wide-band filters.

Even the coaxial resonant cavity becomes inefficient at extremely high frequencies where the Q factor has to be in the order of several thousand to satisfy the filter design (the higher the frequency, the higher the required Q factor). Therefore, for narrow-band filters, a different kind of resonant cavity is used which is essentially a piece of waveguide separated by partitions. Waveguide cavities are physically larger and more efficient. Like any other closed cavity with conducting walls, an infinite number of discrete resonant frequencies exist, each corresponding to a different configuration of electromagnetic fields within the interior of the cavity. At any one of these resonant modes, the cavity is, in many ways, like an ordinary resonant circuit and its behavior may be described in terms of three ordinary resonant circuit parameters—center frequency, Q factor, and characteristic impedance. However, for each possible resonant mode, these parameters generally will have different values. A resonant waveguide cavity and its single mode equivalent circuit is shown in Fig. 5c.

The increasing use of the microwave range has demanded continual advances in circuit technology. For example, one new type of circuitry is the stripline filter. This multiple-coupled resonator band-pass filter is made in half-wavelength strips coupled end to end or, alternately, in parallel, as shown in Fig. 6. Parallel coupling offers several important advantages over end coupling. For example, the length of the filter is reduced, and a much larger gap is permitted between adjacent strips. This last advantage is of particular importance, because it permits a broader bandwidth for a given tolerance, and permits a higher power rating.

Building Blocks

The electric filter, at relatively low frequencies (up to 100 mc), can be easily realized as a combination of simple building blocks called sections. Each of these blocks is a certain canonic combination of lumped reactances. At microwave frequencies these reactances are distributed, but for the purpose of analysis, they can be reduced to an equivalent schematic with lumped components.

A low-pass elementary lattice structure and its equivalent forms are shown in Fig. 7a. The form in the center is a bridged-T schematic, and the form on the extreme right is the semilattice or differential bridge filter. (The low-pass filter with a transformer, such as the differential bridge, is a low-pass filter only in a limited sense because it does not pass direct current.)

A high-pass elementary structure in lattice form, and the equivalent ladder schematic, is illustrated in Fig. 7b. Similarly, a band-pass filter in a lattice form and its ladder equivalent is shown in Fig. 9.

Although the lattice is the ideal form of filter, it is highly uneconomical. It consists of repetitive elements and consequently is seldom used. But, being the most general type of building block, it theoretically permits the realization of a more universal response than any of its partial equivalents. The conditions of effective transmission for any lattice filter are very simple; the arm reactances (series and parallel arm) must be opposite in sign. As soon as the two arm reactances have the same sign (both capacitive or both inductive) the filter starts attenuating.

The single building block of a filter produces one peak of attenuation at f_∞. The lattice filter can be realized with a peak on either side of the passband. The ladder equivalent schematic with positive element values can be realized with a peak on only one side. However, under certain con-

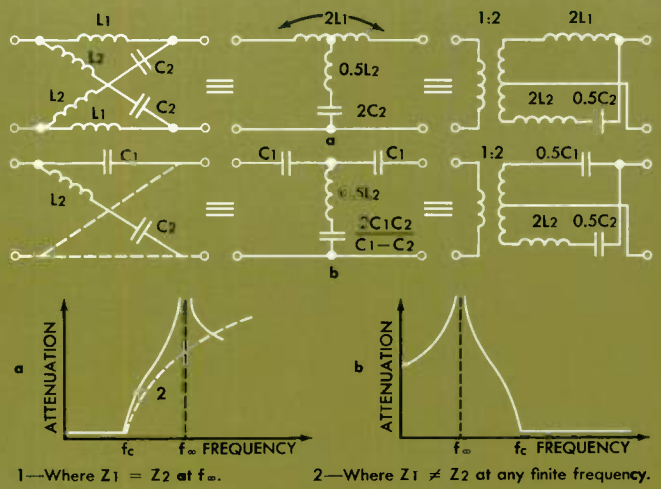

Fig. 8 Typical attenuation curves for (a) the low-pass lattice filter and (b) the high-pass lattice filter shown in Fig. 7.

Fig. 7 (Left) Lattice filters and their equivalent forms: (a) Low-pass lattice filter, an equivalent bridged-T ladder (equivalent if the elements are positive), and semilattice or differential bridge; (b) high-pass lattice filter and its equivalent (equivalent for positive elements) forms.

Fig. 9 (Below) A typical lattice band-pass filter and its ladder equivalence (equivalent when the elements are positive) and corresponding attenuation curve. (Repetitive elements shown by dotted lines.)

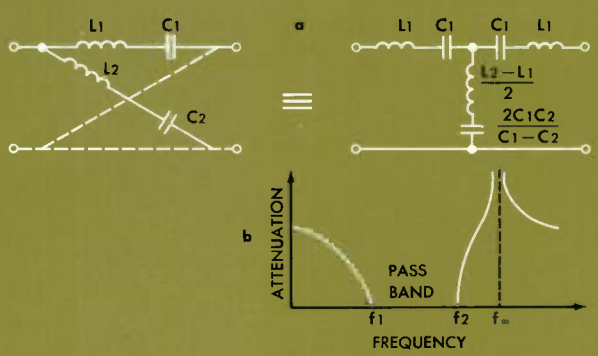

ditions, one element in the shunt arm of the ladder section can be made to disappear. For example, in the case of Fig. 9a, the shunt inductance may be zero. The filter's response on both sides of the passband will then be smooth without any peaks of attenuation.

Composite Filters

A combination of several building blocks is required to provide a desired filter response. The *conventional* composite filter, ladder or lattice, consists of many half-sections in tandem. The sections should be of the same characteristic impedance if they are designed according to the image impedance theory. In the *polynomial* filter, the composite filter is described by an *n*th-order polynomial where *n* is the minimum number of reactive elements. The element values are the result of continued fraction expansion of the polynomial and appear to be of the same physical structure as a conventional filter. The essential difference between polynomial and conventional filters is that polynomial filters are not iterations of sections in the classical sense and cannot be subdivided into sections.

Four half-section filter blocks connected in series are shown in Fig. 10a. A polynomial filter consisting of four coils and four capacitors obtained from an eighth-order polynomial is shown in Fig. 10b.

Because of its economical use of low-Q inductors, the unconventional pass-band filter* is the most popular type of filter at present. Three typical unconventional filter sections (Note: the last is the same as the first.) are shown in Fig. 11. For many situations, the unconventional filter sections can be synthesized into a composite filter to obtain the desired overall filter characteristics. An example of the synthesis process is shown in Fig. 12. The total amplitude and phase response of unconventional filters is equal to the sum of partial responses, but the shape of responses are dependent upon the position of the peaks of attenuation outside of the pass band.

Problems of Design

In electronic design, gain is usually cheap but selectivity is expensive. Therefore, a major effort is required to find the most rational way to design a network with the minimum number of expensive components, and at the same time, satisfy the fundamental physical problems of attenuation, phase, etc. The mathematical problem consists primarily of finding a network whose transfer function fits the appropriate polynomials, or more generally, a ratio of polynomials. In most cases these functions are of the Chebyscheff** type, which provide the best and the most elegant solution. Using such functions, not only the shape of the gain or amplitude response can be organized in a

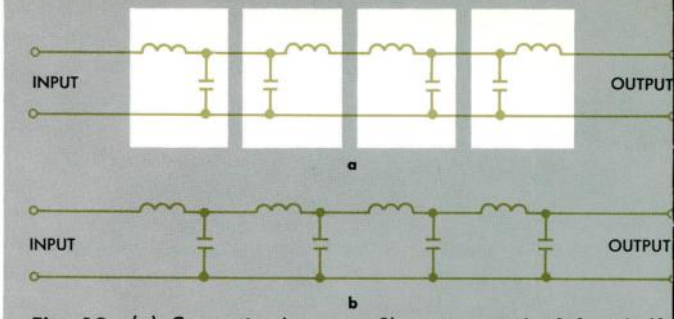

Fig. 10 (a) Composite low-pass filter composed of four half-sections. (b) Eighth-order polynomial low-pass filter.

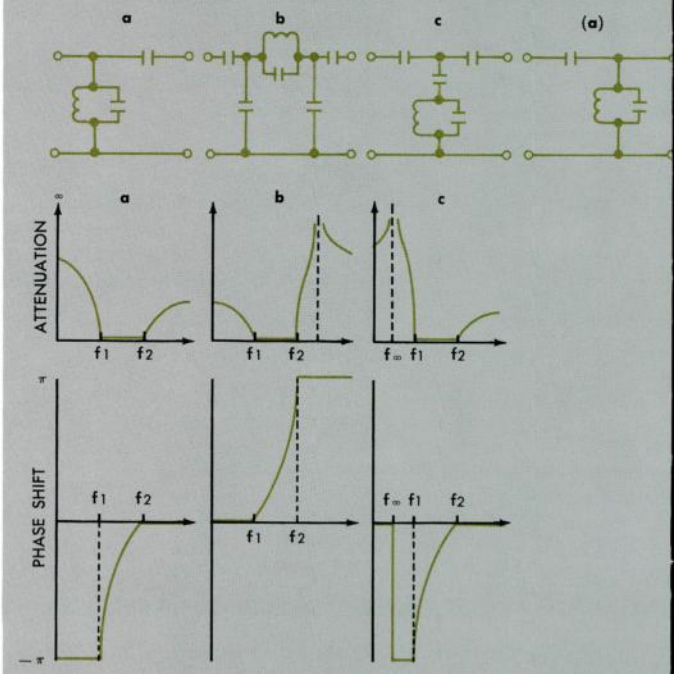

Fig. 11 Three typical unconventional pass-band filters are shown with their respective attenuation and phase-shift curves. These are the most popular types of filters at present.

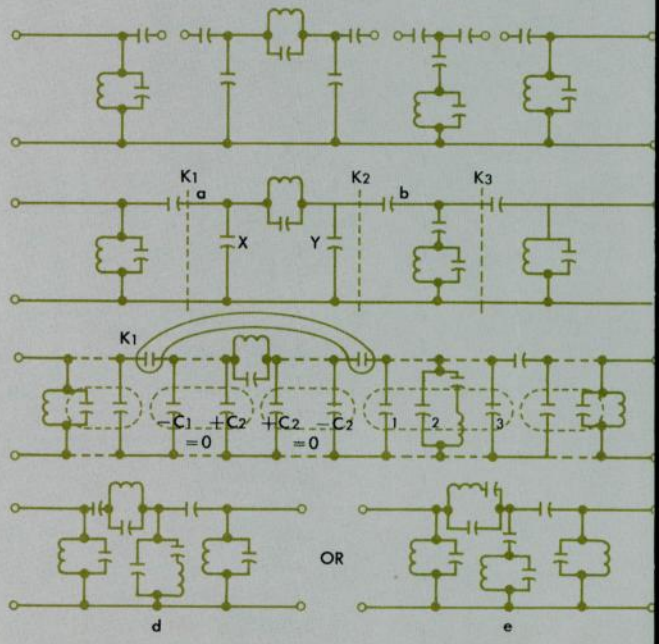

Fig. 12 (Right) To illustrate the synthesis process, four elementary blocks (from Fig. 11) are connected together to produce one monolithic block-filter. The second step shows the intermediate step in the synthesis procedure. K_1, K_2, and K_3 shows where ideal transformers can be incorporated to produce a capacitor π out of C_a and C_x etc. The third step shows the resulting capacitive π's and how the negative capacitors and other capacitor combinations can be matched together to avoid redundancy. The fourth step shows the final synthesized filter. Hence, the final version consists of 4 coils and 7 capacitors instead of 4 coils and 13 capacitors. A similar procedure can be used for lattice filters.

specific form, but even the shape of group delay distortion or a specific type of phase response can be designed.

Amplitude Response—Many different shapes of amplitude versus frequency response can be described by analytic functions. Design procedures have been established to approximate these types of amplitude responses. There are several distinctive varieties but only three will be discussed here: 1) Butterworth response, or the "maximally flat" pass band; 2) Chebyscheff response (with "equal ripple" attenuation in the pass band); and 3) Gaussian response. The Butterworth and Chebyscheff responses are the most familiar and the most popular among filter designers. Some other typical response types are: elliptic, Bessel response, or "maximally flat delay" filters, equal ripple delay filter response, Legendre filters, and synchronously tuned (multiple-pole filters).

The "maximally flat" amplitude response is called Butterworth after the British physicist who developed the type of polynomial. This response corresponds to that obtained with the critically coupled condition of the double-tuned circuit (Fig. 13). It may be described as response with a single maximum in the center of the pass band and an attenuation outside of the pass band which increases as rapidly as possible (Fig. 14a).

The equal ripple response, usually called the Chebyscheff response, corresponds to that obtained with the overcoupled condition of the double-tuned pass-band circuit (Fig. 13). This shape possesses several ripples of equal height (Fig. 14b). The number of ripples is equal to the number of reactive elements (low-pass filter), or number of resonant circuits (band-pass filter) used. The low-pass equal-ripple filter for a given bandwidth and ripple has a greater attenuation outside of the pass band than the Butterworth filter. The rate of increase depends not only upon the number of resonators, but also upon a special design parameter, the height of the ripple. Attenuation is higher when the pass-band ripples are greater.

The Gaussian response is represented by the well-known exponential formula***. This filter is a compromise for use in pulsed systems where, except for the frequency discriminations, faithful reproduction of the pulse shape is important. (The rate of increase in attenuation for Gaussian, Bessel, and equal-ripple delay filters usually is very low.) Typical amplitude discrimination shapes for the Butterworth, Gaussian, and Bessel responses are shown in Fig. 15.

In filter technology there are many other types of amplitude responses (for example, nonsymmetric responses) that cannot be described easily by analytical functions. These filters require different design techniques, and have different requirements for element values, and different component technology.

Phase and Group Delay Response—A specific amplitude response does not describe the complete transmission property of a filter. Indeed, the phase characteristic of a network becomes very important for radar and communica-

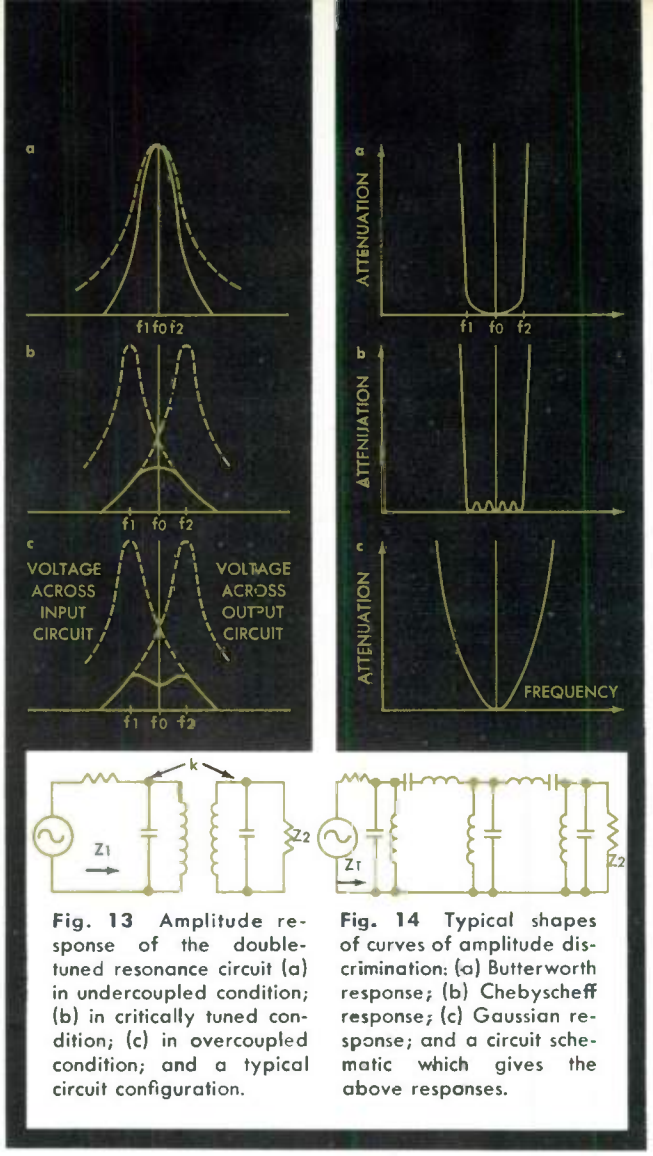

Fig. 13 Amplitude response of the double-tuned resonance circuit (a) in undercoupled condition; (b) in critically tuned condition; (c) in overcoupled condition; and a typical circuit configuration.

Fig. 14 Typical shapes of curves of amplitude discrimination: (a) Butterworth response; (b) Chebyscheff response; (c) Gaussian response; and a circuit schematic which gives the above responses.

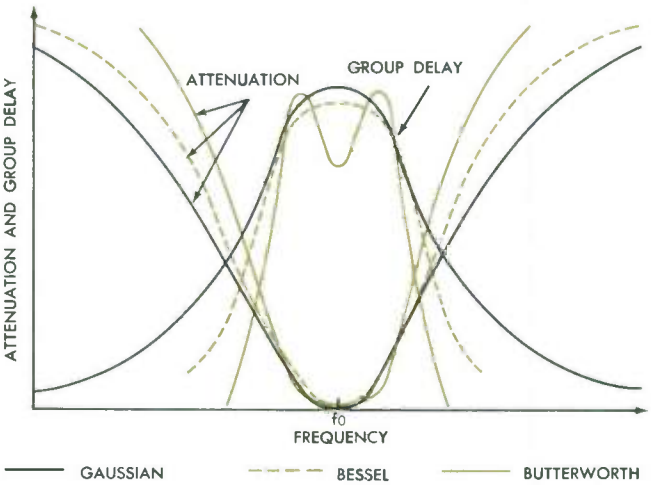

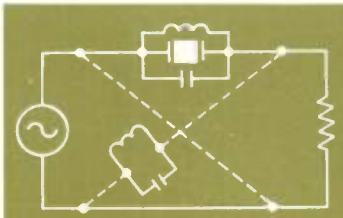

Fig. 15 Amplitude and group delay response curves for a Bessel, Gaussian, and Butterworth filter, each with two resonators.

*For the present discussion an unconventional pass-band filter is defined as one which is made up of building blocks each of which contains only one inductor (or capacitor) and two or more capacitors (or inductors).

**Named for the 19th Century Russian mathematician.

***The ideal Gaussian shape $H_\omega = e^{-a\omega^2}$ where a is a constant and ω is the frequency variable.

tion apparatus using pulsed systems. Usually the requirements are that rapid signal changes must not generate large over- or under-shoots (damps oscillation or ringing).

The phase response of the ideal Gaussian filter is linear, and no overshoots will be produced as a result of rapid signal changes. Realizable low-pass equivalent Gaussian magnitude filters with a finite number of resonators yield nonsymmetrical pulse responses because the phase response is not sufficiently linear. The trailing edge of the output pulse is longer than the leading edge.

Another amplitude response that is important from the phase point of view is the Bessel amplitude response, which is described by a Bessel polynomial. The phase response of a Bessel filter with a finite number of resonators is more linear than the corresponding Gaussian filter. The skirt of selectivity of the pass band is sharper, the ratio of attenuation at cutoff for both filters is not very great. They are both very poor filters with regard to cutoff rate, but from the point of view of group delay distortion or phase characteristics their pulse responses, in comparison with Chebyscheff or Butterworth, are remarkably good.

The group delays of Bessel, Gaussian, and Butterworth filters are plotted in Fig. 15 for purposes of comparison. Note that the group delay of the Bessel filter is flat at the center of the pass band. A flat group delay is desirable because this signifies that all frequencies will be delayed the same amount while going through the filter. If the various frequencies are not equally delayed, dispersion results and the output does not retain its original wave shape.

Some Filter Applications in Electronic Equipment

The use of electric wave filters in electronic equipment progresses as equipment becomes more complex until almost all of the individual operations in the various equipment rely upon filters. Some typical filter functions are the following:

Preselector Filters—This type of filter is required at the input (front end) of all sensitive receivers to separate the desired signal or signals from the unwanted signals. Because the desired signal is always low in amplitude while the undesirable signals, including noise, may be appreciably greater, the preselector must have a low insertion loss to the desired signal and high attenuation to undesirable signals. Such a filter may be either of the Gaussian or Chebyscheff type.

SSB Filters—In contrast to the very symmetrical preselector filter, the single-sideband filter for a modern communication scheme requires nonsymmetrical attenuation on opposite sides of the pass band; indeed, the filter in such a scheme becomes the heart of the system. Sometimes, instead of a filter, phase difference networks are used to eliminate the unwanted sideband. In either case the purpose of the network is to suppress the second sideband to such a degree that it does not contribute appreciably to the amplitude distortion and instability of the received signal.

Comb Filters—The optimum filter can extract a predetermined signal from a medium where noise is prevalent or jamming is introduced. In general, the optimum filter is a device whose input consists of a signal representing the mixture of information-bearing signal and noise. At the output of this same filter, only a signal closely approximating the useful signal will be present. This is a most important application of information theory. For a signal represented by a periodic series of pulses, such an "optimal" filter will be a "comb" filter which consists of a chain of narrow-band filters passing spectral lines over the frequency spectrum of the signal. It passes discrete frequency components and discriminates against noise. Such filters are generally Gaussian.

Multiplexing Filters—These filters provide multiple use of a broad frequency spectrum beam between terminal stages of a radio relaying system. It is possible to create up to one thousand telephone channels in one microwave link. In the case of a wire carrier communication network the frequency range extends from the audio band up to 200 kc (the same for power-line communication). The use of coaxial lines widens the range of frequencies and more communication channels can be created. The one requirement of such a filter is to obtain the sharpest possible attenuation outside of the pass band to suppress cross talk between channels; hence a Chebyscheff filter is applicable here.

Antijamming Filtering—Artificially created noise for jamming can completely destroy the target signal if no antijamming features are incorporated in a radar system. To improve target detectability, some special features are created which feature the narrow-band filter. The primary requirement is that the filter operating with pulsed signals has not only selectivity but also minimizes overshoots and ringing. To satisfy this requirement, the steady-state response curve of the filter usually has to be of Bessel or Gaussian shape.

Matched Filters are the cornerstone of a new science—correlation techniques and time domain filtering. These filters are used for generation and detection of chirp signals, which have been widely used in radar applications for target identification. Chirp signals are prolonged pulse envelopes of frequency-modulated waves having a frequency that changes continuously in one direction without reversal. All-pass passive filters generate this type of pulse. Chirp signals can be used in communications to transmit binary data. Marks and spaces can be coded by corresponding ascending and descending frequency-modulated pulsed envelopes.

Matched filters in the above case provide a spectrum spreading technique, and can make effective use of any band width, tolerate large distortion, be insensitive to noise, tones or spurious signals, resist jamming, operate with single sideband frequency translation or Doppler shift, reject impulse noise, provide good signal-to-noise ratio, and require no synchronization. Areas of application include teletype, signaling field data, and various data entry systems.

Only a small part of the great variety of electronic filters and their applications have been mentioned here. The sophisticated problems in the field of interference, telemetering guidance, industrial control systems, etc., reduce themselves to the problems of frequency or time discrimination. That is why the most wanted component in electronics industry today is an electronically tunable filter. The recent advancement in tunnel diodes, varactor diodes, and microwave ferramics in combination with inductors, capacitors and other resonators opens many new avenues for filter development and filter applications.

about the authors

J. K. Dillard, a regular contributor to these pages, joins forces with a new coauthor, **E. W. DuBois,** to discuss extra-high-voltage transmission. Dillard, manager of the Electric Utility Engineering Department, is an EE graduate of Georgia Tech and has an MS degree from MIT. He joined Westinghouse in 1950, after three years on the Electrical Engineering Department staff at MIT.

Earle W. DuBois holds a BS in physics from Holy Cross College (1948), an MS in electrical engineering from MIT (1950), and an MBA from New York University (1957). He came with Westinghouse on the Graduate Student Program in 1950. By 1952, he had completed the Consulting and Application Engineering Training Program and was assigned to the New York office as a C&A Engineer. In 1958, he was made a Sponsor Engineer in the Electric Utility Engineering Department and assigned to the Pacific Coast Zone. DuBois' special fields are generator excitation systems and long-distance high-voltage transmission.

Anatol Ivan Zverev was born and educated in Russia, where he earned a Diploma Engineering degree (MS) from the Leningrad Electrotechnic Institute and a Candidate of Technical Science (PhD) from the Academy of Transport in Moscow.

In 1938, he became Chief Communication Engineer of the Russian Ministry of Transportation, and was primarily engaged in designing and installing the first carrier telephone line across Siberia. He joined the Russian army as a Signal Officer in 1941, and attained the rank of Captain before his capture by the German army in 1942 near Kharkov.

He was freed by the American Third Army at Munich in 1945, and shortly thereafter became Director of the International Professional School in Munich.

In 1947, Zverev decided to move to Belgium. He worked in a Belgian coal mine while preparing for the professional engineer's examination at the University of Louvin. After passing the exam, he became a senior design engineer in the Belgian firm, Ateliers de Constructions Electriques de Charleroi.

Zverev came to the United States in 1953, and shortly thereafter, joined the Westinghouse Electronics Division as a senior engineer, to work on the development of filters for power line carrier communication systems and other special circuits. Over the past ten years, Zverev has worked on passive network design for communication, radar, data-transmission, and satellite navigation systems. He is section manager of network synthesis at the Electronics Division.

Zverev's outside interests include chess, philosophical literature, gardening, fishing, and teaching. One particular accomplishment is language—Zverev can speak fluently in Russian, Polish, German, French, and English. He insists that until recently, he spoke English like a Frenchman—but the transition is finally complete now that he can "think" in English.

E. J. Borrebach has worked with electrical and control equipment for metallurgical furnaces—arc, induction, resistance, and basic oxygen—ever since he joined Westinghouse in 1950. His work and his interests are process-oriented, dealing with the characteristics and capabilities of various furnaces and with automatic operation and computer control of the processes that use those furnaces. He is a sponsor engineer in the Industrial Systems Metals Province, responsible for application of electrical and control systems to furnaces. He has contributed to many engineering developments in this field, including the control system for the basic oxygen process described in this issue.

Borrebach earned his BS in electrical engineering at Tufts College in 1950 and immediately joined Westinghouse on the Graduate Student Course. He is also a graduate of the Westinghouse Electrical Engineering Design School and is a member of the Association of Iron and Steel Engineers and the American Institute of Metallurgical Engineers.

Like most engineers in the nuclear field, **James H. Wright** began his career in a totally different technical area, and then migrated to nuclear engineering.

Wright graduated from Texas Technological College in 1948 with a degree in chemical engineering. He promptly embarked on a career in the oil industry. He joined the Gulf Oil Corporation in their production division, where he served as a chemist, and later as plant engineer and assistant plant superintendent. In 1952, he was awarded a petroleum fellowship at Mellon Institute of Industrial Research.

In 1956, Wright joined the growing ranks of nuclear engineers; he became a fellow engineer in the reactor physics section of the Westinghouse Atomic Power Division. In 1958, he became manager of Advanced Reactor Systems, where he has the responsibility for planning, implementing, and directing the reactor technology development program for advanced concepts.

During this period, Wright managed to earn his master's (1954) and doctor's (1957) degrees in chemical engineering at the University of Pittsburgh.

Wright has also found time for a variety of outside activities; among others, he is chairman of a cub scout pack, a deacon in his church, and participates in local choral productions. He is also an avid shutterbug, and a flier—of radio controlled model airplanes, that is.

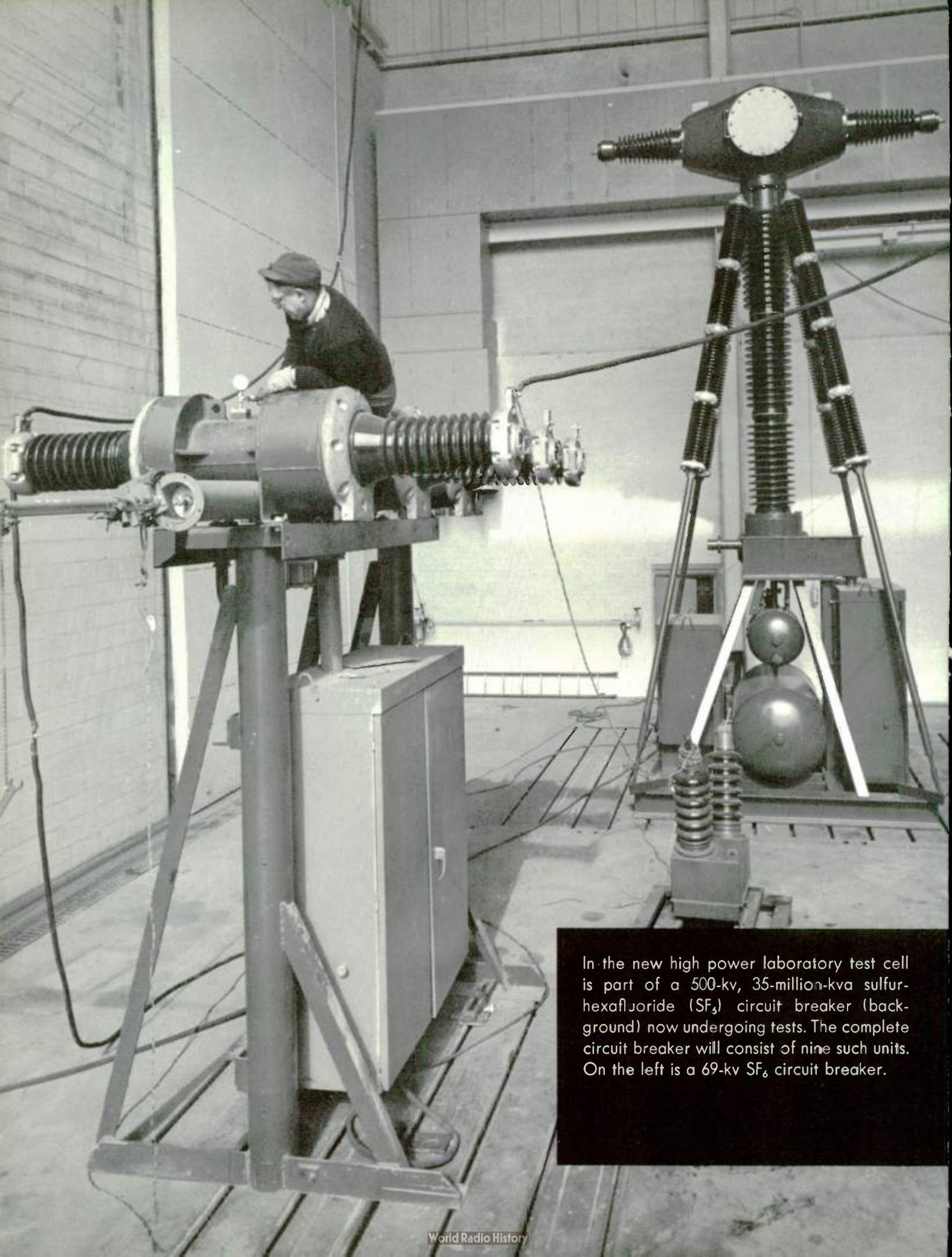

In the new high power laboratory test cell is part of a 500-kv, 35-million-kva sulfur-hexafluoride (SF_6) circuit breaker (background) now undergoing tests. The complete circuit breaker will consist of nine such units. On the left is a 69-kv SF_6 circuit breaker.